FUNDAMENTAL MODELLING OF REACTING FLOW IN RAMJET DUMP COMBUSTORS

J.C. DUTT

NOVEMBER 1980

REPORT DOCUMENTATION PAGE

READ INSTRUCTIONS BEFORE COMPLETING FORM

1. REPORT NUMBER: AFOSR-TR-81-0597	2. GOVT ACCESSION NO.: AD-A102 554
3. RECIPIENT'S CATALOG NUMBER	
4. TITLE (and Subtitle): FUNDAMENTAL MODELLING OF REACTING FLOW IN RAMJET DUMP COMBUSTORS	5. TYPE OF REPORT & PERIOD COVERED: ANNUAL Rept. 01 Jan [illegible] - 30 OCT. '80
6. PERFORMING ORG. REPORT NUMBER	
7. AUTHOR(s): J.C. DUTT	8. CONTRACT OR GRANT NUMBER(s): AFOSR-80-0174
9. PERFORMING ORGANIZATION NAME AND ADDRESS: UNIVERSITY OF SHEFFIELD, MAPPIN STREET, SHEFFIELD, S1 3JD. U.K.	10. PROGRAM ELEMENT, PROJECT, TASK AREA & WORK UNIT NUMBERS: 61102 F 2308/A2
11. CONTROLLING OFFICE NAME AND ADDRESS: AIR FORCE OFFICE OF SCIENTIFIC RESEARCH/NA, BUILDING 410, BOLLING AIR FORCE BASE, DC 20332	12. REPORT DATE: November 1980 13. NUMBER OF PAGES: 52
14. MONITORING AGENCY NAME & ADDRESS (if different from Controlling Office)	15. SECURITY CLASS. (of this report): UNCLASSIFIED 15a. DECLASSIFICATION/DOWNGRADING SCHEDULE: N/A

16. DISTRIBUTION STATEMENT (of this Report)

Approved for public release; distribution unlimited.

17. DISTRIBUTION STATEMENT (of the abstract entered in Block 20, if different from Report)

18. SUPPLEMENTARY NOTES

19. KEY WORDS (Continue on reverse side if necessary and identify by block number)

Mathemat ical Modelling	Combustion Efficiency
Combustion Model	Recirculation Zone
Turbulence Model	Reattachment length
Dump Combustors	Predictions
Finite-Difference Algorithm	Experimental data

20. ABSTRACT (Continue on reverse side if necessary and identify by block number)

The calculated results based on the universal two-equation model known as k-ε model of turbulence for recirculating, reactive and non-reactive flows in dump combustors (12" ID) are presented extending the previous results obtained in this Department. The experimental data on the combustion efficiency, flow fields and recirculation zones for such combustors from the Air Force Aero Propulsion Laboratory, Ohio and the Arnold Engineering Development Centre, Tennessee have been compared with those predicted by the present modelling procedure and found to be in remarkably good agreement.

DD FORM 1 JAN 73 1473

unclassified 400047

SECURITY CLASSIFICATION OF THIS PAGE (When Data Entered)

FOREWORD

The work reported herein was conducted at the Department of Chemical Engineering and Fuel Technology, Sheffield University, U.K. on behalf of the Air Force Office of Scientific Research (AFOSR), U.S.A. and forms the continuing effort of evolving a mathematical modelling method which can be used as a viable design technique for ramjet dump combustors.

This report forms the second stage of such an effort and highlights the capabilities and requirements for further development in the model and computer programme by comparing the predicted flow fields and combustor performance characteristics with the experimental results available from the works done at the Air Force Aero-Propulsion Laboratory (AFAPL), Ohio, and at the Arnold Engineering Development Centre (AEDC), Tennessee.

The report covers work performed during the time period of February 1980 through December 1980.

This work was carried out under the overall supervision of Professor J. Swithenbank of the Department whose guidance, help and encouragement are gratefully acknowledged.

The author also wishes to thank the AFOSR for supporting and financing the work.

1. INTRODUCTION

This report represents an extension and refinement of the previous report[1] with the specific aim to further develop and validate the numerical modelling technique so that predictions which may be directly compared with the experimental results may be obtained for tubulent, ducted, subsonic, axisymmetric, recirculating, reactive or non-reactive flow systems typically encountered in a dump combustor.

The present research project was performed for the Air Force Office of Scientific Research (AFOSR), U.S.A. In the previous report, the details of the mathematical models comprising physical modelling, turbulence modelling, thermodynamics modelling, radiation modelling and chemical kinetics which characterise the flows in combustors were given. The essential features of the Computer Programme for solving the partial differential equations by the finite-difference method were also reported there and will not be repeated here for the sake of brevity.

The preliminary results obtained for a sudden expansion dump combustor showed that the Computer Programme had some deficiencies when the combustion in the chamber was considered. Typically, it predicted the temperature distribution (Fig. 31 in reference (1)) for both diffusion and pre-mixed flames with peak values being centred near the centre-line of the combustor. The mathematical model presented therein was recheked and the fault was traced in the computer programming itself. This has since then been corrected and the results reported here will show that the modifications and corrections introduced in the computer programme have improved the capability of the prediction method. The predicted mean axial and radial velocity, mean kinetic energy of turbulence and dissipation rates and the temperature profiles are more plausible and agree very well with the experimental results (2-6) for dump combustors.

The design and development studies (2-5) at the Air Force Aero Propulsion Laboratory, Ramjet Technology Branch, Ohio have established several novel requirements for the successful operation of ramjet missiles. This advanced generation of strategic and tactical missiles have, as their integral parts, the rocket-ramjet such that the rocket booster and the ramjet engine operate as a completely integrated system. This introduces the constraints that the missiles must be volume limited.

The basic combustor cofiguration experimentally studied at AFAPL, is illustrated in Fig. 1 which is the so-called sudden-expansion dump combustor. In this system fuel can be pre-mixed or injected from the wall in the inlet air-stream, upstream of the sudden expenaion step. Primary flame stabilization is achieved by the recirculation region just downstream of the dump station. Additional flame stabilization with subsequent higher combustion efficiency can be achieved by mechanical flame holders placed at the air inlet-dump station interface. Combustion efficiencies in excess of 90% can be obtained and studies at the AFAPL have established that for small diameter combustors (> 0.1270 m ID) high blockage flameholders and combustor length-to-diameter ratio , L/D ≈ 6.0 are required while for larger combustors (∿ 0.3048 ID) comparable combustion efficincies can be obtained for L/D = 3. In the larger combustors, the severe pressure losses found in the case of shorter combustors with flameholders are avoided. However, the study of Craig et al (2) showed that the larger combustors can attain still higher efficiencies for equivalent blockage, if some pressure loss is tolerated. The studies by Craig et al (4) also showed that the mode of fuel entry (wall injection or pre-mixed), the types of flameholders (annular, y-shaped) and the inlet temperature, all influence the combustion efficiency. However, it was found that for higher efficiencies, L/D = 3 or more is required. Other important results were that both higher inlet temperature and the incorporation of additional flameholders give higher combustion efficiencies, η_c. Furthermore, it was found that in

the case of a pre-mixed flame, higher η_c was obtained for higher fuel-to-air ratio, f/a, whilst in the case of fuel injection from the wall the highest efficiencies were obtained at a lower f/a ratio with an almost linear decrease in η_c with increasing f/a ratio. The annular wedge type flameholders did not follow the same consistent trend found with the Y-type flameholders and showed less sensitivity to f/a ratio and L/D ratio.

In view of the vast amount of results available from the experimental investigations on the parametric variations of the basic co-axial dump combustor performance, it was obvious that the analytical models can be tested and if validated can be used as an additional tool for the design of ramjet combustors and other flow configurations which are encountered in a wide variety of engineering applications.

2. BASIC COMBUSTOR CONFIGURATION

The basic coaxial dump combustor configurations which were chosen for the modelling purposes are shown in Figs. (2a, 2b) and relate to the 0.3048 m ID combustor tested by Craig et al (2). Fig. 2a refers to the sudden expansion type dump combustor and does not incorporate the flameholders and exhaust nozzle section. Fig. 2b incorporates these two aspects into the sudden expansion dump combustor and also differs from Fig. 1 in the following respect, i.e. the fuel enters premixed with the inlet airstream. The combustor shown in Fig. 2a has been studied by a two-dimensional Computer Programme (TEACH), while that shown in Fig. 2b has been studied by a three-dimensional Computer Programme based on the SIMPLE algorithm, both of which were originally developed at Imperial College, London. However, numerous refinements and modifications have been made at Sheffield University in the physical modelling and computer Programme to incorporate the features found in dump combustors.

The ranges of other parameters which have been investigated in the present study are given below and conform very closely to those ranges given by Craig et al (2).

Combustor L/D = .3 to 5

Inlet velocity, U_{in} = 180 to 240 m/s

Inlet pressure = 1.15×10^5 N/m^2

Combustor inlet temp., T_{in} = 600 K

Fuel/air ratio, f/a = 0.03 to 0.065

Fuel used = JP-4

Reynolds number, R_e, based on the primary flows at the inlet duct is calculated from,

$$R_e \sim \frac{D_{in} \cdot U_{in}}{\nu} \sim 1 \times 10^6 \sim 1.2 \times 10^6 \qquad (1)$$

It is a well known observation that at such a value of R_e, the time-averaged velocity, species concentrations, static pressure fields, etc. become independent of R_e which is the case in the present study (N.B. the flow is fully turbulent at this value of R_e).

The chemical properties of the fuel which have been used in the reactive case studies are given below. (Private communication[7].)

Fuel : JP-4 ($C_{9.5}$ $H_{18.9}$)

Density : 762.457 Kg/m^3

Viscosity : 9.584×10^{-4} Kg/m.s

Heat of combustion (H_{fu}) : 43.49×10^6 J/Kg

Molecular weight : 133.15

Specific heat, C_p : 2.031×10^3 J/Kg.K

3. MODELLING OF COLD FLOW: TWO-DIMENSIONAL ANALYSIS

While the difficulties, as mentioned earlier, in the three-dimensional numerical computer programme were being investigated, the numerical modelling programme based on TEACH was modified in order to apply it for predicting the recirculating ducted flow systems pertaining to the dump combustor configurations as shown in Fig. 2a.

A. CASE-STUDY I-2D: WITHOUT BAFFLE

The following are the details of the geometry and boundary conditions adopted in this case. It is to be noted here that these b.c.s also apply to all the cases which will be presented in this report, unless mentioned otherwise.

(a) Geometrical Features

The geometry adopted is a simple sudden expansion dump combustor (Fig. 2a).

Length of the combustor : 1.29 m

Length of the inlet section : 0.1695 m

Diameter of combustor, D_D : 0.3048 m

Diameter of the inlet section, D_{in} : 0.1524 m

(b) Boundary Conditions

(i) Initial flow boundary specification

Inlet air velocity : 220 m/s

Pressure : 1.01×10^5 N/m^2

Temperature at the inlet : 300 K

Density : 1.2 Kg/m^3

(ii) Modelling of κ and ε at the inlet

The kinetic energy of turbulence, κ, at the inlet was taken as

$$\kappa_{in} = 0.03 \cdot U_{in} \qquad (2)$$

The corresponding turbulence dissipation rate, ε, was taken as

$$= \frac{\kappa^{3/2}}{0.002 \times D/2} \qquad (3)$$

The turbulence model used in the present study, it is to be noted, is given by

$$\mu_t = \rho C_D \kappa^2/\varepsilon \quad (C_D = 0.9, \text{ a constant}) \qquad (4)$$

= turbulent or effective viscosity

(c) Exit Plane

The static pressure is assumed to be uniform and constant. The axial gradients of all the remaining variables at the exit plane are set to zero.

(d) Axis of Symmetry

The radial gradients of all the variables excepting v are set to zero.

(e) Wall Boundaries

Wall shear-stress, τ_s is required for the boundary conditions of the momentum equations and for the evaluation of the κ-generation term.

In the previous report[1], the b.c. for the momentum equations were set to be the components of the wall-shear-stress in the direction of the velocities - and an empirical correlation formula relating the shear-stress coefficient ($C_f \sim 0.03$) with Reynolds number was used to evaluate the wall shear-stress τ_s.

Similarly, for κ and ε, Γwall for κ was set to zero since κ has small diffusion near the wall while ε was set equal to:

$$\varepsilon = C_D^{\frac{3}{4}} \kappa^{3/2} / \mathbb{K} \delta \qquad (5)$$

where $\mathbb{K} = 0.43$ (Von Karman's Constant)

δ = the distance of the wall from the nearby grid nodes.

However, in the present study, the 'Log-law of the wall' given by Spalding (8) has been used and is detailed below.

Assuming a constant shear region near the wall, τ_s is obtained via a modified Log-law:

$$U_+ = \frac{1}{\mathbb{K}} \ln (E\, y +) \qquad (6)$$

where $E = 9.73$ for smooth wall

Now,

$$\Gamma\text{wall} = \frac{1}{\tau_s} \frac{du}{dy} \quad \text{for u-component} \qquad (7)$$

Where τ_s is obtained for this range of y^+ from

$$\tau_s = U_{\text{near wall}} \, (\rho \, C_D^{\frac{1}{4}} \, \kappa^{\frac{1}{2}}) / [\ln(EY^+)/\kappa] \tag{8}$$

and $$Y^+ = \rho \, \kappa^{\frac{1}{2}} \, C_D^{\frac{1}{4}} \, \delta / \mu_L \tag{9}$$

(μ_L = laminar viscosity)

The expression for Γ_{wall} for a general variable comes from the "$\phi^+ = \sigma_{eff} \, (u_+ + P)$" - type of 'the law of wall'. The quantity, P is calculated from:

$$P = 9.0 \, (\sigma/\sigma_{eff} - 1) \, (\sigma/\sigma_{eff})^{\frac{1}{4}} \tag{10}$$

The following table shows the wall functions used for different variables:

Table I

ϕ	Γ_{wall}
(1) Velocity component normal to the wall	0
(2) Velocity component parallel to the wall	$Y^+ > 11.63$: $\dfrac{\mu_L Y^+}{u_+}$ $Y^+ < 11.63$: μ_L
(3) κ	0
(4) ε	$C_D^{\frac{3}{4}} \, \kappa^{3/2} / \kappa \, \delta$

(f) Computational Parameters

(i) Grid structure

A 20 x 20 grid in the axial and radial directions was used with a greater number of grid nodes being concentrated near the sudden expansion region.

(ii) Under-relaxation parameters

In order to achieve stability and avoid divergence in the numerical solution method, the following under-relaxation parameters were used for the different variables:

Variable (ϕ)	Under-relaxation factor (α_ϕ)
u	0.2
v	0.2
P'	1.0 (i.e. no under-relaxation on P')
κ	0.5
ε	0.5
μ	0.5

(iii) Convergence test

The iteration process is monitored by comparing the sum of the absolute values of residual mass sources in the field with a preset value as given below:

$$[(\text{Sum of absolute residual mass sources}) \times \dot{m}_{inlet}] < 10^{-6}$$

B. CASE STUDY II-2D: WITH BAFFLE

The geometry adopted for this case study is shown in Fig. 2a with the baffle flameholder placed at the interface of the inlet-sudden expansion step, similar to that shown in Fig. 2b. The flameholder used is an annular wedge type (i.e.V-gutter)similar to that used by Craig et al (4) and gives a blockage of $\sim$ 10% at the inlet port.

The governing equations solved and the b.c. employed are similar to those given above in case study I-2D.

RESULTS AND DISCUSSION

The convergence characteristics for the two cases are shown in Fig. 3. The residual mass imbalance less than 10^{-4} was obtained after about 350 iterations in Case Study I-D while in the second case less than 150 iterations

were needed to reach the same extent of convergence, showing that fully developed turbulent flows are achieved quicker with the baffle.

Fig. 4 illustrates the essential features of the recirculating flow field. The recirculating zone is developed near the sudden expansion region due to the production of turbulent eddies with high turbulent intensities and relatively low average backflows. The flow is characterized by viscous interaction between the channel like flow, A, and large quasi-steady viscous region B. The recirculating eddy structure disappears after a short distance downstream of the dump station and the duct flow is characterised by positive axial velocities throughout the velocity field. The recirculation zone with the reattachment point is also shown in the figure.

The reattachment length for such a ducted recirculating flow field has been the subject of a number of experimental studies (5, 6, 9, 10) and will be discussed in detail later on (viz. section 4.(c)) to show that the reattachment distance is correctly predicted by the present numerical method.

The representative radial distributions of mean axial velocity and mean radial velocity are shown in Figs. 5 and 6 - for the two cases - at a number of axial positions upstream and downstream of the dump station. In Fig. 7 are plotted the mean axial velocity profiles for these two cases for the sake of comparison. Fig. 8 shows the mean turbulent kinetic energy in radial directions at a number of axial positions. The axial distribution of the centre line velocity is shown in Fig. 9. The data in these figures excepting Fig. 8 have been non-dimensionalised by the inlet velocity, U_{in} and the axial and radial distances have been ratiodd to the dump combustor duct diameter. The kinetic energy profiles are non-dimentsionalised by the inlet kinetic energy, K_{in}.

The marked differences in the profiles for the two cases are apparent in the figures. These will now be discussed. The velocities in the recirculation zones are higher when the baffle is present. This is also supported by the

higher turbulent kinetic energy profiles as shown in Fig. 8. The maximum value of normalised turbulence kinetic energy κ/κ_{in} is reached closer to the sudden expansion plane. The maximum values occur near the centre of the mixing zone and extend further downstream. However, the positive axial velocities are smaller in magnitudes but more uniform when the baffle is present. The decay of the centre line velocity is higher with the baffle than without the baffle, showing the higher mixing achieved in the former case.

These features are in broad agreement with the experimental results of Smith et al (6).

4. 3-DIMENSIONAL ANALYSIS: REACTIVE AND NON-REACTIVE FLOWS: WITH OR WITHOUT BAFFLE AND NOZZLE

The computer programme capable of solving 3-dimensional partial differential equations was modified and improved to remove the difficulties mentioned earlier. The programme was then applied to a number of simple cases and was found to give plausible predictions. The results which will be reported in this section relate to the dump combustor configurations shown in Fig. 2b.

The geometrical dimensions ofthe dump combustor and in the case of reacting flows, the fuel used are given in section 2.

A 27 x 18 x 7 grid structure in the x, y and θ-direction was chosen. The differential equations solved are u, v, P', κ, ε for the non-reactive case and u, v, P', κ, ε, f, m_{fu} and h in the case of reacting flows. The differential equations for these variables, their significance and meaning are to be found in reference 1.

RESULTS AND DISCUSSION

(a) CASE STUDY I-3D: WITHOUT FLAME HOLDER OR NOZZLE

The radial distributions of the mean axial and radial velocities for the reacting case are shown in Figs. 10(a,b), while the mean axial velocity distributions for the non-reactive case are shown in Fig. 11(a,b). The axial distribution of the centre line velocities for both reactive and non-reactive cases are shown in Fig. 12.

The data shown for radial profiles of velocities (Figs. 10, 11) at a number of representative axial locations clearly demonstrate that the heat release due to chemical reaction broadens and enhances the radial profiles. It is also evident that considerable non-uniformities in the velocity profiles remain evan at X/D ∿ 4.9 in the reactive case while in the non-reactive case the profiles become essentially uniform at X/D ≈ 3.6. The uniform distributions at X/D ≈ 1.5 for both cases are also to be expected as thic location is at a considerable distance upstream of the dump mixing and recirculation zone and downstream of the inlet port.

The data shown in Fig. 12 also shows in conformity with the radial velocity profiles that the velocity decays less rapidly in the reacting case than in the non-reacting case.

All these predictions agree reasonably well with the experimentally observed data of G.D. Smith et al (6). These experimental results were obtained for a sudden expansion dump combustor made of 1.524 m long stainless steel duct with an inside diameter of 0.133 m and hence correspond closely to the actual dimensions used in the present predictions. This close agreement is shown in Fig. 11(c).

Figs. 13(a,b) show the predicted radial and longitudinal velocity vectors for the cold flow case study. The recirculation zone with the backflow vectors near the step height expansion plane and the more axial positive velocity profiles far downstream and near the exit plane are evident in these figures.

(b) CASE STUDY II-3D: WITH FLAME HOLDER AND EXHAUST NOZZLE

Two types of flameholders or baffles have been studied - the rectangular orifice ring, Fig. 14(a,b) and the annular wedge type, Fig. 2b. Only cold flows have been simulated with the rectangular orifice ring type baffles whilst both cold and hot flows have been studied in the case of annular wedge type baffles, as these type of baffles have been the subjects of experimental studies[4,5].

Figs. 14(a,b) show the radial and longitudinal velocity vectors for the cold flow system when rectangular orifice type baffles are used. The flows past the rectangular baffle placed at the interface of inlet-sudden expansion plane and the exhaust nozzle clearly show the channel like flow and the back-flows in the viscous region just downstream of the baffle and dump station.

The convergence characteristics are shown in Fig. 3 and demonstrate similar behaviour to those mentioned earlier.

The radial distribution of mean axial velocity profiles for the non-reacting case with an exhaust nozzle and annular wedge type flameholder are shown in Figs. 15 and 16. The addition of the nozzle alone or nozzle plus the baffle alters the profiles profoundly as can be seen from the comparison of the data in Figs. 8 through 16. The data for the axial decay of the centre line velocities both for cold and hot flows for a number of such cases are shown in Fig. 12.

The addition of the baffle increases the mixing near the dump station but the axial locations where the profiles become uniform or fully mixed are advanced towards downstream locations. The expansion of mean axial velocity along the centre line (Fig. 12) due to the presence of chemical reaction is similar to the experimental observations by Smith et al (6) and Wang et al (11).

Figs. 17(a,b) show the radial distribution of mean axial and radial velocities for the reactive case when both the annular type of flameholder and exhaust nozzle (Fig. 2b) are present. The data presented in Figs. 15 through 17 demonstrate the effect of chemical reaction and heat release on the profiles. It clearly shows that heat release broadens the radial profiles and highlights the sustained higher velocity resulting from the chemical reaction as observed in experimental studies (6).

Fig. 17(c) shows the radial distributions of axial velocities and temperatures for the reacting case and should be compared to the data shown in Fig. 16 for the non-reacting case. Axial velocity profiles are similar except

that the magnitudes of the velocities are nearly twice as big in the former case due to the effects of chemical reaction.

(c) DISCUSSION OF THE FLOW RECIRCULATION ZONE AND REATTACHMENT LENGTH

The recirculation zones and the reattachment lengths in the flowfield just after the sudden expansion dump station are shown in Figs. 4, 5, 7 and others presented in the previous sections. It can be seen that the flow separation characteristics are well defined for both reactive and non-reactive cases. There are a number of experimental studies of this zone relevant to the dump combustor configurations (4, 5, 6, 9, 10, 12). It is therefore worthwhile and interesting to compare the present predicted zones with those experimental observations.

Fig. 18, shows the variation of recirculation zone lengths L', with sudden expansion stepheight, h, for a number of axisymmetric, ducted turbulent mixing combustor flow systems. The combustor duct diameter, D has been used as a normalising parameter. In this figure are shown the experimentally observed variations of L'/D with h/D as well as those predicted by the present numerical simulation method.

Based on the surface oil flow visualization results, Drewry (5) found that that there are two linear relationships for the variation of reattachment length L' with the step-height, h, as given below

$$L' = 7.9\ h \qquad (11)$$

and

$$L' = 9.2\ h \qquad (12)$$

The slight difference in the dependency of L' on h was attributed to the differing Reynolds number. However, the results of Smith et al (6) showed that this length, L' may also depend on whether chemical reaction is present or not, while Chriss (13) and Schulz (14) found that L' is essentially

identical for the reactive and non-reactive case.

Similarly, the results of experimental observation by Abbott et al (9) showed no variation of L' or flow patterns for wide ranges of Reynolds number ($\sim 10^4 - 10^6$) and turbent intensities, provided the flow is turbulent before the step, which is true for all the cases studied in this report.

Table II shows the flow recirculation zone length, L', for a number of cases which have been studied by the present modelling technique. It can be seen from the table and Fig. 18 that the predicted reattachment length mostly follow the relation given by equation (12) and the results from reactive and non-reactive case studies show that L' is essentially the same for both cases in conformity with the results of Drewry (5), Chriss (13) and Shulz (14).

However, comparisons of the cases (a) through (e) in table II show that the variation of L' may depend on h/D ratio being less than 0.25 or so. This may be caused by the fact that when h is less than the radius of the inlet port, R_{in} (Fig. 18), the mixing zone is reduced and attains a more or less constant value when the step height is of the order of the radius of the inlet port. In this context, the results of Abbott et al (9) are noteworthy.

Abbot et al observed that the flow separation in sudden expansion chambers has three distinct regions - laminar, transitional and turbulent. In the laminar case, the flow is laminar all the way beyond reattachment. In the transitional stall, the flow is laminar at separation but transition to turbulent flow occurs prior to reattachment. In the turbulent case, the boundary layer is turbulent before the separation. However, these three distinct zones which exist in the recirculation region, cannot be distinguished by the present computer programme because of the limitations which have to be put on the grid structure.

Abbott et al showed that L'/R_{in} plotted against h/R_{in} gives a better and consistent dependence of the reattachment length on the combustor geometry. Accordingly in Fig. 19, the lengths L_1' and L_2' corresponding to the transitional

TABLE II: FLOW RECIRCULATION ZONE LENGTHS FOR DIFFERENT CASES

Combustor	Flow Conditions	L'	D	h	h/D	L'/D
Sudden Expansion only	Cold	0.6721	0.3048	0.0762	0.25	2.21
	Cold					
	Cold (a)	0.6350	0.2920	0.0698	0.24	2.20
	Cold (b)	0.4255	0.2794	0.0635	0.23	1.52
	Cold (c)	0.3302	0.2660	0.0568	0.214	1.31
	Cold (d)	0.2540	0.2540	0.0508	0.20	1.0
	Cold (e)	0.642	0.3048	0.0762	0.25	2.10
	Cold	0.632	0.3048	0.0762	0.25	2.07
Sudden Expansion with Annular Wedge baffle	Cold	0.664	0.3048	0.0762	0.25	2.12
Sudden Expansion with Annular Wedge baffle and Exhaust Nozzle	Cold	0.580	0.3048	0.0762	0.25	2.0
Sudden Expansion with Exhaust Nozzle only	Hot(f/a = 0.05)	0.5750	0.3048	0.0762	0.25	2.0
Sudden Expansion only	Hot(f/a = 0.05)	0.617	0.3048	0.0762	0.25	2.02
	Hot(f/a = 0.05)	0.175	0.0762	0.0191	0.25	2.29
	Hot(f/a = 0.045)	0.692	0.3048	0.0762	0.25	2.27
	Hot(f/a = 0.055)	0.692	0.3048	0.0762	0.25	2.27
	Hot(f/a = 0.04)	0.692	0.2048	0.0762	0.25	2.27
	Hot(f/a = 0.35)	0.692	0.3048	0.0762	0.25	2.27

and turbulent regions normalised by R_{in} are plotted against h/R_{in}. The predicted values from the present calculation are also plotted in the figure. It can be seen from the figure that Abbott's result show different dependence of L_1' and L_2' on h beyond about $h/R_{in} > 0.5$ or so. Hence they have been drawn as a band in the figure and the predicted values fall within this band. The values on the dotted curve in Fig. 18 have been replotted in Fig. 19, which incidentally shows that L'/R_{in} against h/R_{in} gives a better representation of their dependence than L'/D against h/D.

(d) DISCUSSION OF THE PREDICTED TEMPERATURE AND COMBUSTION EFFICIENCY

The modelling of the aerodynamic and thermal behaviour in combustors under combustion has been slightly changed in the present study, compared to that presented in the previous report(1). In turbulent flows, the influences of turbulence on the reaction rates were taken by Spalding's (8) Eddy Break-up (EBU) model where the reaction rate is given by

$$R_{fu,EBU} = - C_R \, g^{\frac{1}{2}} \, \rho \, \varepsilon/\kappa \qquad (13)$$

Here C_R = a constant

$g^{\frac{1}{2}}$ = Local mean square concentration fluctuation

In the previous report, it was assumed that 'g' can be related to the mean concentration of fuel by

$$g^{\frac{1}{2}} = m_{fu} \text{ (= mass fraction of fuel)} \qquad (14)$$

In the present report, a differential equation for 'g' as given below has been solved (15)

$$R_{fu} = - C_R \, C_g \, \rho \, \kappa^{\frac{1}{2}} \left\{ \sum_{i=1}^{3} \left(\frac{\delta m_{fu}}{\delta_{xi}} \right)^2 \right\}^{\frac{1}{2}} \qquad (15)$$

where C_g = a constant of the order of 6.

The representative values of the radial distribution of mean temperature at a number of axial positions are shown in Fig. 20. In this figure the temperature for a sudden expansion dump combustor with or without nozzle are shown. The temperature profiles for a combustor having an annular wedge type flameholder and an exhaust nozzle are shown in Fig. 17c.

The radial distributions of the mean m_{fu} - the mass fraction of unburnt fuel are shown in Fig. 21. This result was obtained with a nozzle at the exit.

The distribution of the temperature profiles are reasonable and in very good agreement with the experimental profiles of Smith et al. The centre line temperature is low and the radial profiles show increasing temperature towards the duct wall to some peak value in the turbulent mixing, recirculating zone region. The downstream station radial temperature profiles are relatively uniform and flat and are consistent with the fully mixed fuel/air ratio, if one takes into account the heat loss to the wall. More uniform temperatures are predicted when both the baffle and nozzle are present (Fig. 17c).

The axial distributions of the centre line temperature and off-centre-line plane (Y/R_D = .23) are shown in Fig. 22. It is instructive to note that the convergence of the centre line values of the flowfields are very slow due to the peculiarities of the solution procedure using cylindrical polar co-ordinate systems. Thus it takes a large number of iterations to obtain fully convergent centre line values while the off-centre-line values reach fully convergent profiles rapidly. This is seen from the fact that the θ-grid spacings decrease towards the centre line, so that a much finer θ-grid spacing exists near the centre line. These smaller spacings cause the f.d.e. coefficients to be much larger than in the other directions (x and r-directions) coefficients. Because after the TDMA (ref. 1) traverse in x and r-directions, the resulting variable near the centre line at any θ-plane is influenced by the neighbouring values of the variable at the previous and subsequent θ-planes and since one of the neighbouring values will always be the previous iteration

value and the other, though a new iteration value, will still be very close to the previous iteration value, the initial guessed near centre line values are being updated very slowly. This behaviour is clearly demonstrated in Fig. 22. The curves I, II and III for centre line temperature profiles are drawn after 100, 200 and 400 iterations respectively while the curve V is drawn after 100 iterations and IV remains constant upto 400 iterations. Thus it shows that while the centre line temperature profile still needs more iteration to adjust to the converged values, the off-centre line temperature profile has already reached the fully converged values. The same behaviour is shown by the centre line axial velocity also.

Fig. 22 also shows that at the axial location X/D ≃ 3 to 4, the off-centre temperature profile has attained a flat value (also shown in Fig. 21) indicating almost fully mixed and burnt condition.

The effect of inclusion of the nozzle on the combustion is shown in Fig. 20. It is seen that the inclusion of the nozzle at the exit enhances the mixing and hence the burning of the fuel with the consequent increase in the chemical reaction and heat release (∿ 2% more temperature rise has been predicted).

The radial distributions of m_{fu} shown in Fig. 21 clearly demonstrate the amount of fuel left and hence the state of chemical reaction and burning. The fuel is nearly spent towards the exit. The increases in the amount of m_{fu} distributions towards the ducted wall locations (marked A, B in Fig. 21) correspond to the inlet and the dump station walls where the chemical reaction was deliberately allowed not to take place in the present programme. This is also reflected in the dip in temperature profiles (Fig. 20). This was done in absence of any knowledge of the wall temperature. This information when available could be easily incorporated into the programme. However, in the present computer model any assumed wall temperature can be used and the combustion efficiency could be studied which could not be done here due to lack of computer time.

(e) DISCUSSION OF PREDICTED COMBUSTION EFFICIENCIES WITH THE EXPERIMENTAL RESULTS

A number of parametric studies (2 to 6) relating to the sudden expansion dump combustors having different L, D, h, f/a, T_{in}, etc. have been made experimentally and their effects on the combustion efficiencies found. It is therefore, worthwhile to compare these experimental results with the predictions from the present computer model calculations. This will further add confidence to the ability of the numerical modelling technique as a tool of designing purposes.

Fig. 23 shows the experimental results (16,17) of sudden expansion dump combustors for a number of dump combustor diameters against f/a. These results were obtained for pre-mixed fuel-air entering the combustors at a number of f/a ratios. It is clear from the figure that the combustion efficiency increases with the dump combustor diameter as well as with the f/a ratios.

The combustion efficiency also depends on the combustor length-to-duct diameter ratio L/D for each duct diameter as shown in Fig. 24. The experimental results are shown in Fig. 24. The experimental results are redrawn from Stull and Craig's (16) data. The fuel used was JP-4 (section 2) whose equivalence ratio of 1 corresponds to f/a = 0.0677. The experimental data are for a 0.3048 m ID dump combustor for L/D = 3 and 4.5. These two values of L/D were chosen as the L/D ratio for the calculation falls within these limiting values. The combustion efficiencies predicted by the computer model are also shown in Fig. 24 for a number of f/a ratios.

The experimental combustion efficiency was obtained from

$$\eta_C = \frac{\Delta T_t}{\Delta T_{ti}} \qquad (16)$$

Where ΔT_t is the total temperature rise measured and ΔT_{ti} is the ideal temperature rise for the f/a ratio as computed from equilibrium chemistry calculations.

The predicted combustion efficiency shown in Fig. 24 has been obtained from

$$\eta_C = \frac{\text{theoretical f/a for given } \Delta T}{\text{actual f/a for given } \Delta T} \qquad (17)$$

where ΔT is the rise of temperature across the combustor due to combustion

$$= T_{out} - T_{in}$$

The values of theoretical f/a have been taken from the 'Combustion temperature rise v. f/a ratio' graphs (18) for various values of T_{in}. The reference fuel for which the data has been calculated is a typical hydrocarbon fuel for which the stoichiometric f/a is 0.068 and H_{fu} is 43.1×10^6 H/Hg. These values are very close to those of JP-4 and are thought cerainly adequate for the above calculation. Inaccuracies in the predicted η_C would be less than 1-2% arising from the uncertainties in reading the graphs.

The calculated η_C agrees remarkably well with the experimetnal values of R.R. Craig et al but as can be seen the calculated η_C reaches maximum value and flattens off after f/a $\sim$ 0.06. Hence the model calculation underpredicts the combustion efficiencies over f/a = 0.06.

A major reason for this underprediction of combustion efficiency lies in the use of a simple chemically reacting, one-step global chemical reaction model to characterise the combustion process. Since this model is only an idealisation of what actually occurs, this departure from the observed combustion efficiency is expected. Definitely, better knowledge of the reaction rate constants is required. It is necessary to take into account the multiple reactions in the hydrocarbon fuel combustion process each with its own set of constants. In the present calculation model C_p has been taken as constant. Obviously a temperature and species concentrations dependent C_p would be better.

In future work, these aspects should be incorporated into the model and their effects on the predicted temperature should be studied. (N.B. In our studies of gas turbine combustors, greater precision has resulted from more comprehensive models.) In Fig. 24 also is plotted the calculated η_C when a blockage $\sim$ 10% in the form of annular wedge is placed in the inlet-dump station interface. The experimental studies of Craig et al have shown that the η_C increases with the blockage. Unfortunately, the experimental data are given for only wall injection type of fuel entry and not for pre-mixed flame. Though, as a result, a direct comparison is not possible, an increase of the calculated η_C due to the introduction of a modest blockage is evident in the figure 24. Craig et al have shown that a blockage of 35-40% is needed to see the observable difference in the η_C, which, however, could not be done in the present study due to lack of time. However, in the case of 10% blockage the inlet velocity was 100 m/s while in the case of no blockage, the inlet velocity was 200 m/s. Thus the predicted combustion efficiencies imply that the comparable η_C can be obtained with lower inlet velocity when flameholders are introduced.

Hence a study of the effects of flameholder blockage and the inlet velocity on the combustion efficiency should be undertaken in future work. This presents no problem as the computer programme for these calculations are available and in running condition.

5. CONCLUSIONS: SUGGESTIONS FOR FUTURE WORK

Both reacting and non-reacting flows in a typical sudden expansion dump combustor having 12" ID (0.3048 m ID) have been simulated by a two-dimensional and a three-dimensional computer modelling calculation. The combustor configuration and the inlet flow conditions were similar to those used in the experimental studies conducted at the AFAPL, Ohio, in order to compare the predictions furnished by the numerical modelling technique with those experimental results.

However, due to lack of computer time and the need for extensive modification and development of the existing computer programme, only a small number of parametric investigations could be made.

Only the premixed flames have been studied and reported here. All the investigations are around a 12" ID baseline combustor, with or without flameholders and exhaust nozzle. A number of fuel-air ratios were used in the simulation in order to study the combustion efficiencies, with only one value of combustor length-to-dump-diameter ratio, L/D. Given time, this parametric investigation of different L/D ratios and its effect on the η_C, could be easily conducted with the existing computer programme. This is left for future work.

Two types of flameholders were investigated - one a rectangular orifice type and the other an annular wedge type. Here again, only cold flow studies were conducted in the former case; though in the latter case both cold and hot flows were investigated. The effects of changing the blockage percentages on the η_C were not investigated. This investigation can also be easily undertaken in future work, as the computer programme is in running state and it is only the computer time which is needed.

However, the cold and hot flows in a simple sudden expansion dump combustor as well as in such a combustor with flameholder and exhaust nozzle have been calculated and compared with the experimental data. The predicted values of the flow fields, both reactive and non-reactive, combustion efficiency and the recirculation zone lengths have been found to be in remarkably good agreement with the experimental data.

Only in one aspect was quantitive disagreement observed with experimental data regarding the predicted η_C for f/a ratios nearing the stiochiometric value. The possible reasons for such a discrepancy have been mentioned. It is apparent from experience that combustion of a liquid fuel involves mixing of a fine spray of droplets wirh air, vaporization of the droplets and

intimate mixing of the broken up molecules of the hydrocarbons with the oxygen molecules and finally the combustion process itself. In order to simulate these effects, the one-step chemistry used in the present model is obviously expected to be insufficient to predict the actual temperature rise and hence the real state of combustion in such complicated combustor systems. Two step, or better, multi-step chemistry with temperature dependent C_p should be used and taken up as a future work in this project, together with the inclusion of droplet dynamics.

A further conclusion which can be drawn from this study is that the computer modelling of combustors can add to our knowledge and insight into the factors which affect the combustor performance. The computer modelling technique can with confidence be used to study the detailed behaviour at different regions of the combustor separately and this can be utilized to determine the effects of inlet velcity, temperature, turbulence level, fuel distribution and mode of fuel entry on the overall performance of the combustors and the distributions of the reactants in the combustor flow fields. By judiciously excersizing and altering the states of the inlet flow conditions, fuel-air ratios and distribution and above all geometrical configurations, a large volume of parametric performance informations can be gathered that will aid and cut the cost of 'cut-and-try' experimental work, in the development and design of the dump combustors for various applications.

REFERENCES

1. Dutt, J.C., 'Fundamental Modelling of 3-dimensional 2-phase Reacting Flow Systems', Technical Report, AFOSR-TR-80-0301, 1980.

2. Craig, R.R., Buckley, P.L. and Stull, F.D., Technical Report, AFAPL-TR-76-53, 1975.

3. Chang, C.,Sides, G.D. and Tierman, T.O., Technical Report, AFAPL-TR-76-105, 1976.

4. Craig, R.R., Drewry, R.D. and Stull, F.D., AIAA/SAE 14th Joint Propulsion Conference, Les Vegas, Nev., 1978.

5. Drewry, J.E., AIAA Journal, 16(4), 313, 1978.

6. Smith, G.D. and Giel, T.V., Technical Report, AEDC-TR-79-79, 1980.

7. Stull, F.D., AFAPL, Ohio.

8. Spalding, D.B., 13th Intl. Symp. on Combustion, 649, 1972.

9. Abbott, D.E. and Kline, S.J., Trans. ASME, 84D, 317, 1972.

10. Chaturvedi, M.C., ASCE, J. Hydraulics Divn., 89, 61, 1963.

11. Wang, J.C.F. and Gerhold, B.W., Progress in Astronautics and Aeronautics, Turbulent Combustion, 58, 193, 1977.

12. Pennucci, M.A., Air Force Inst. of Technology, GAE-74S-5, Sept. 1974.

13. Chriss, D.E., AEDC-TR-77-56, AFOSR-TR-77-0749, Sept. 1977, Technical Report.

14. Schulz, R.J., AEDC-TR-76-152, AFOSR-TR-76-108, January 1977.

15. Spalding, D.B., Chem. Eng. Sci., 26, 95, 1971.

16. Stull, F.D. and Craig, R.R., Technical Report, AFAPL-TR-76-15, 1976.

17. Stull, F.D., Craig, R.R. and Hijnacki, J.T., Technical Report, AFAPL-TR-74-90, 1974.

18. Fielding, D. and Topps, J.E.C., 'Thermodynamics Data for the Calculation of Gas Turbine Performance, HMSO No. 3099, 1959.

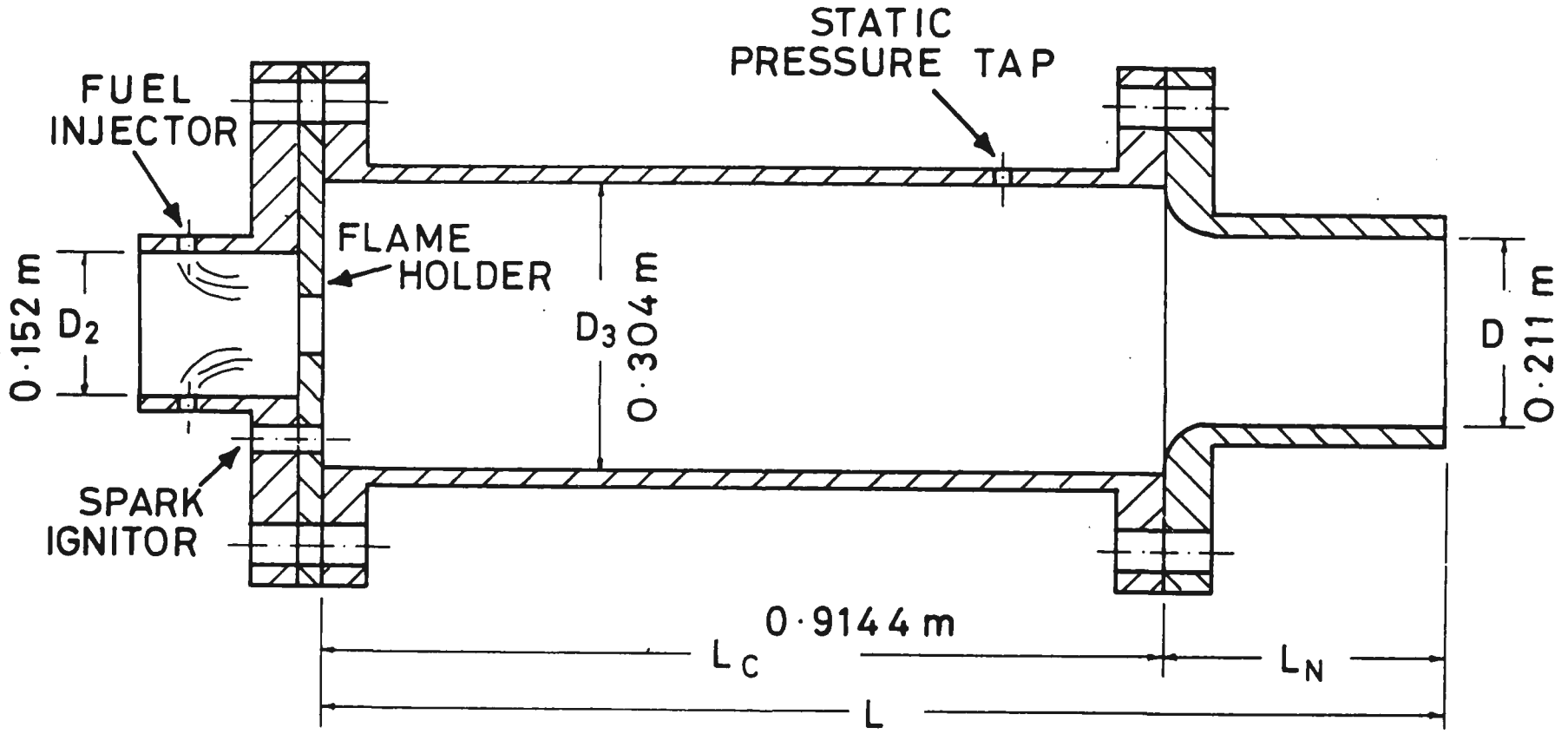

FIG. 1. Dump Combustor with flameholder.

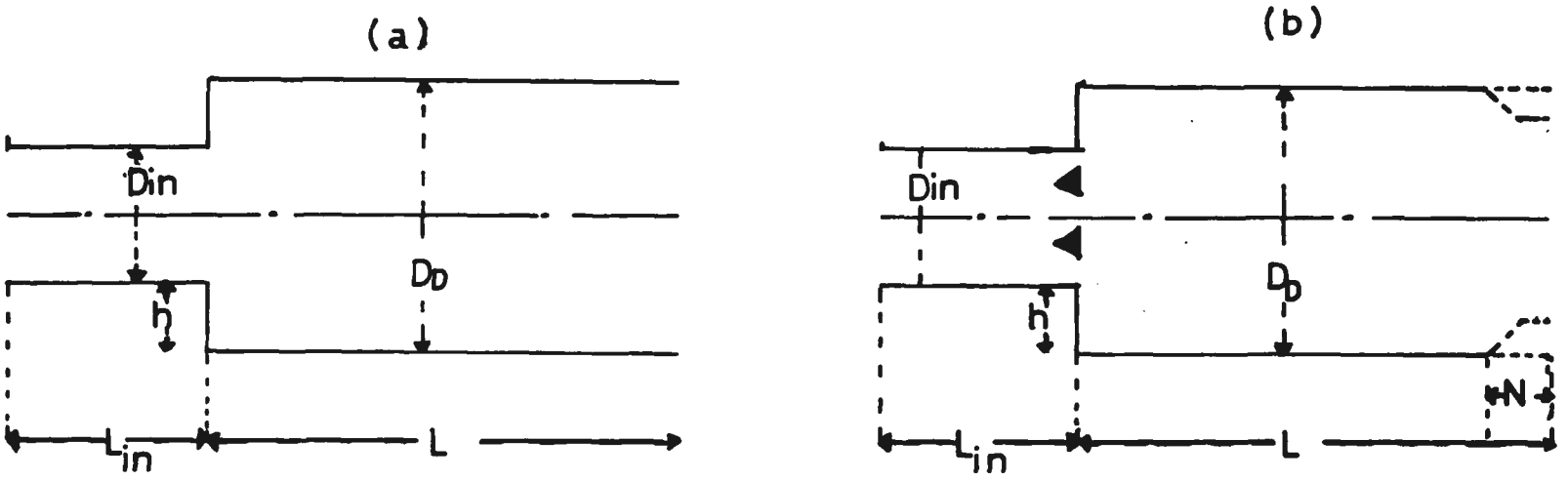

CASE STUDY : 2D

D_{in} = 0.1524 m

D_D = 0.3048 m

h = 0.0762 m

L_{in} = 0.169 m

L = 1.29 m

N = NONE.

CASE STUDY : 3D

D_{in} = 0.1524 m

D_D = 0.3048 m

h = 0.0762 m

L_{in} = 0.24 m

L = 1.28 m

N = 0.019 m

FIG. 2(a). COAXIAL SUDDEN EXPANSION DUMP COMBUSTOR.

2(b). COAXIAL SUDDEN EXPANSION DUMP COMBUSTOR WITH FLAMEHOLDER AND EXHAUST NOZZLE.

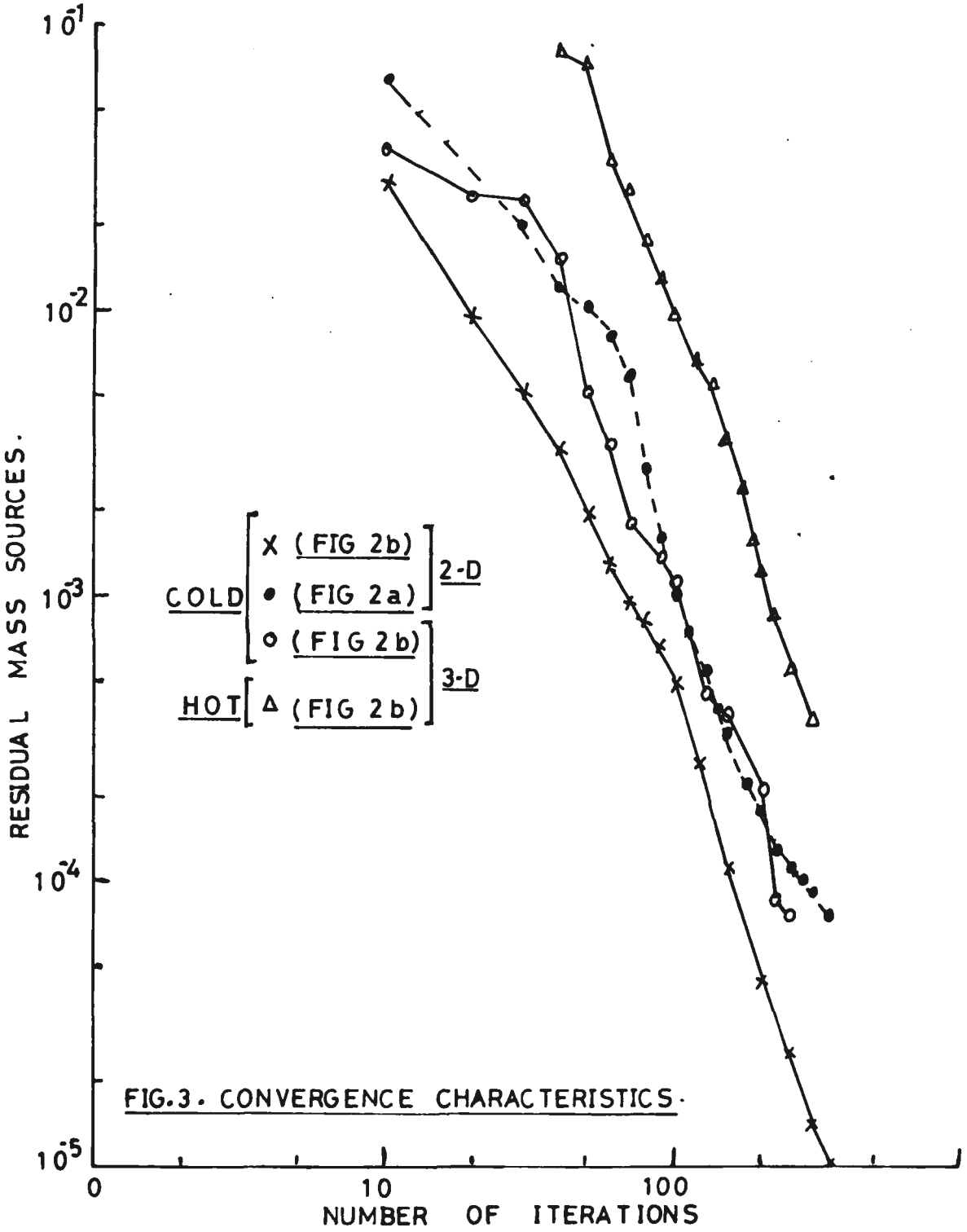

FIG.3. CONVERGENCE CHARACTERISTICS.

L'/h≈ 7.-9.

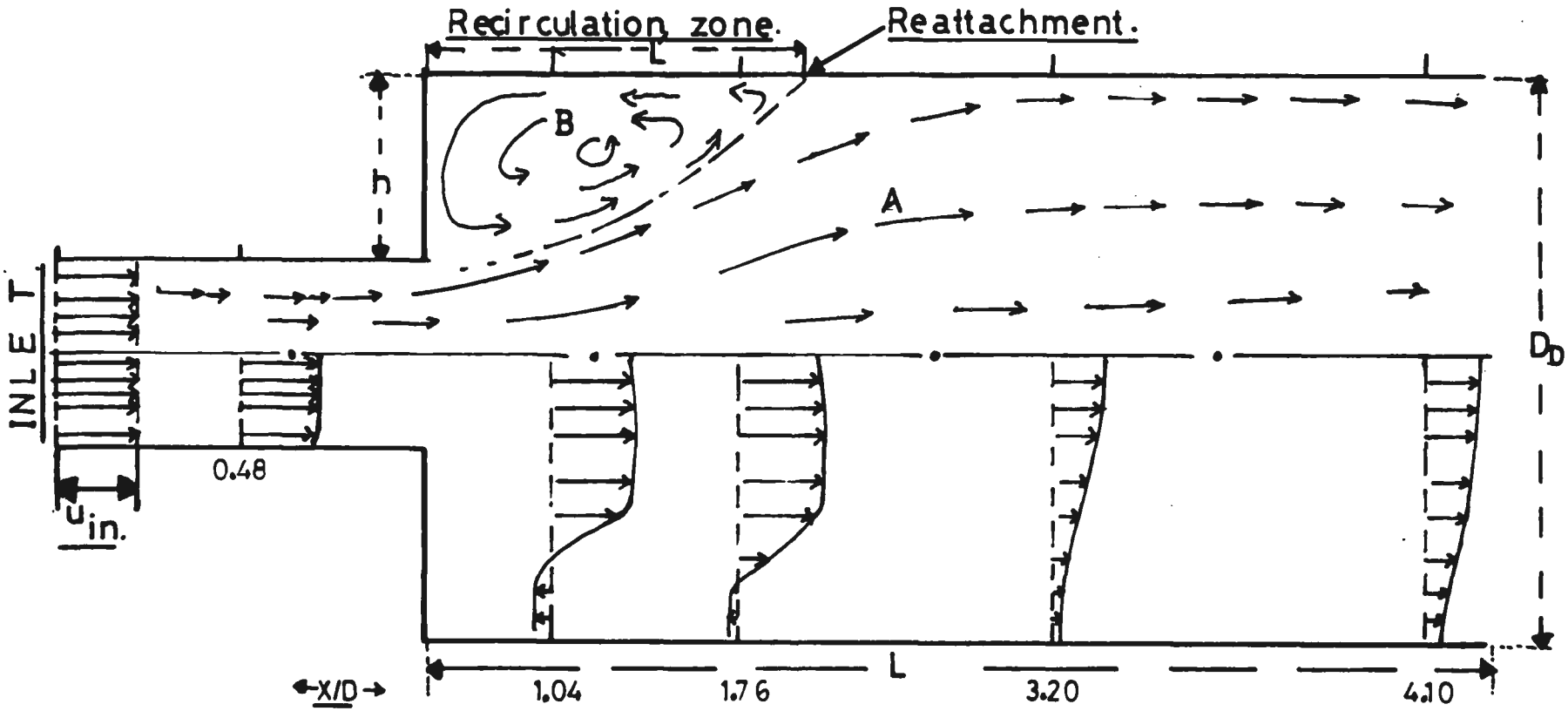

FIG.4. SCHEMATIC ILLUSTRATION OF DUMP COMBUSTOR FLOW FIELD (PREDICTED). Not To Scale.

COLD FLOW (without flameholder).

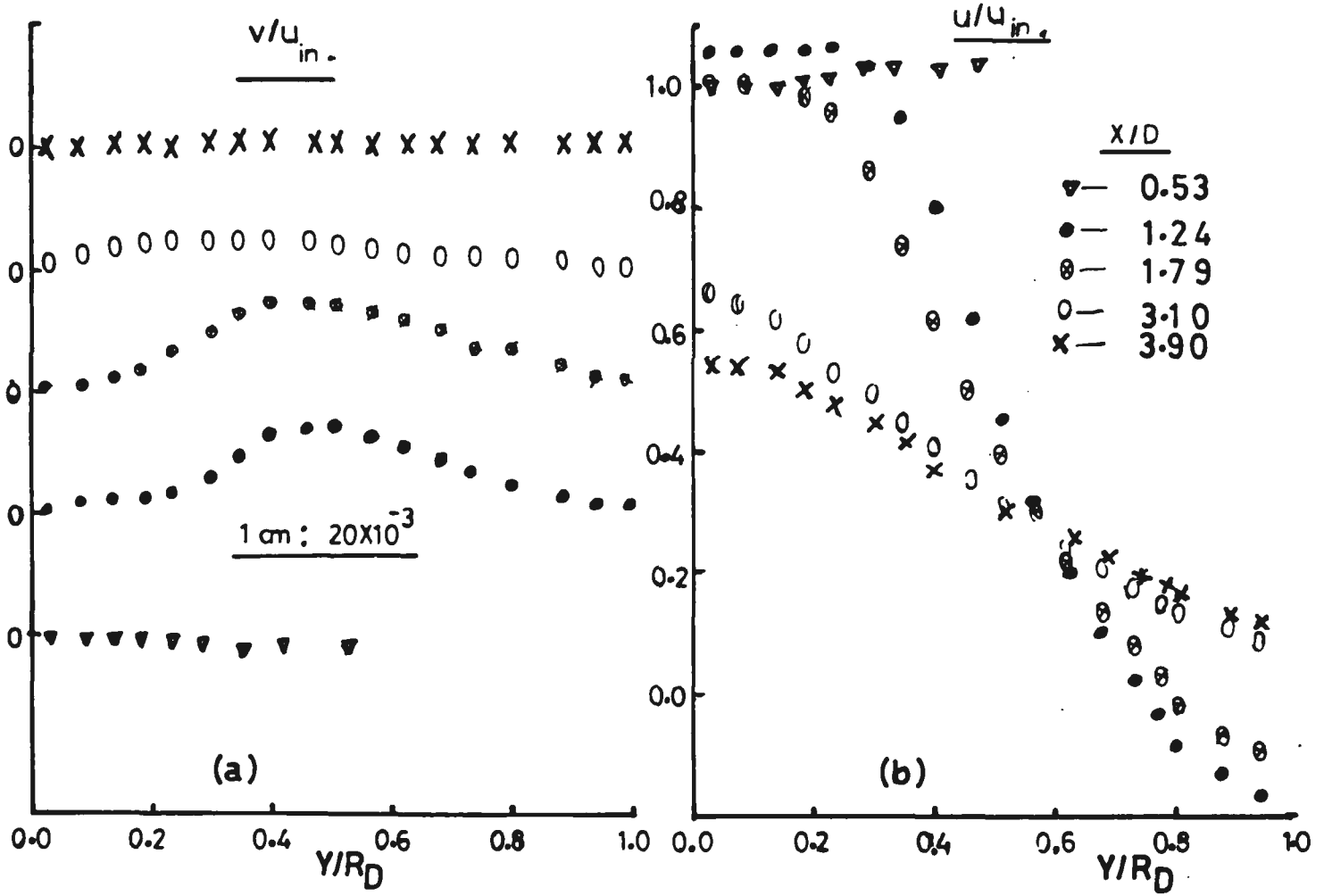

FIG. 5 . RADIAL DISTRIBUTION OF (a) mean radial vel., (b) mean axial vel.

COLD FLOW (with flameholder).

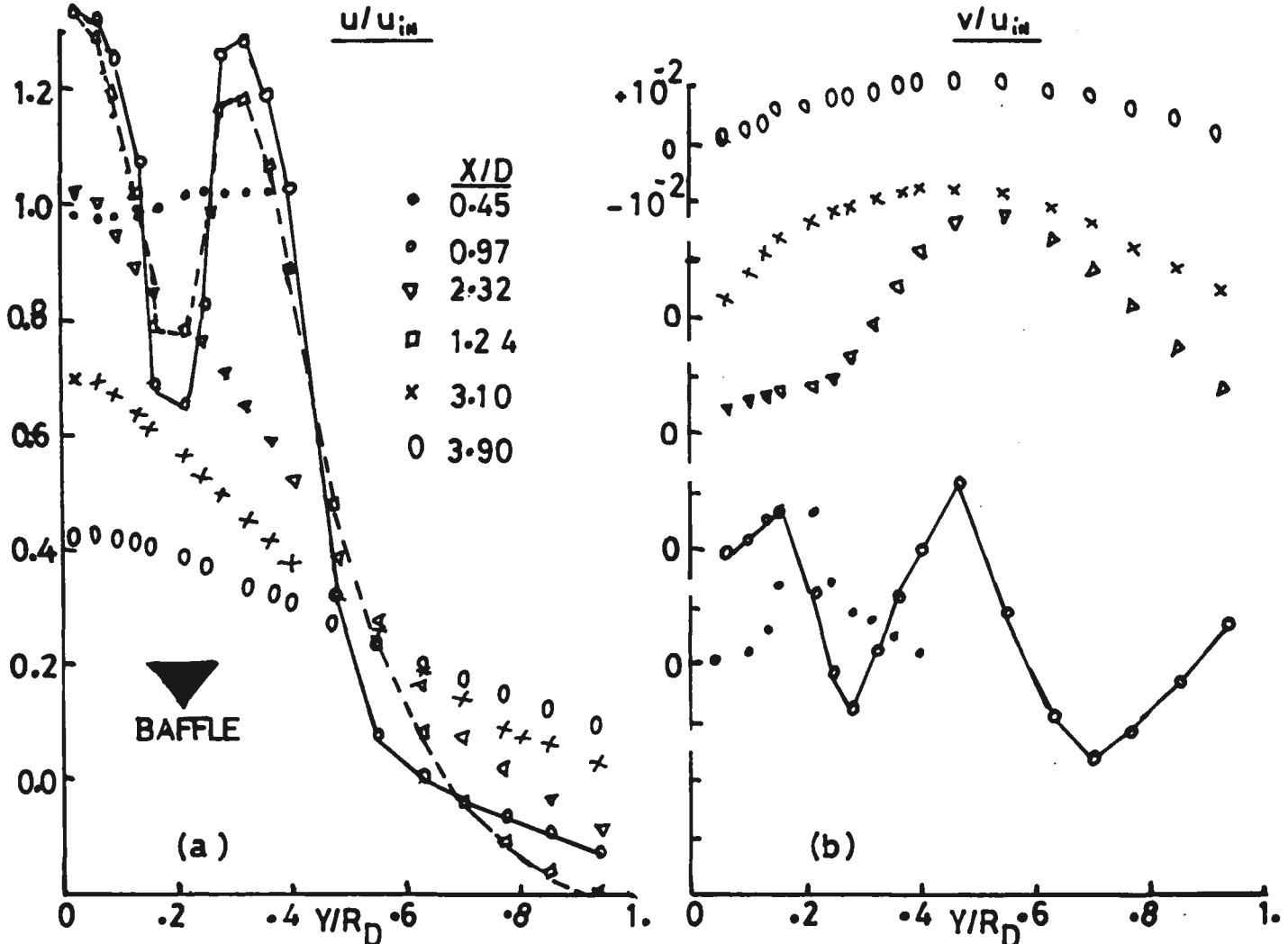

FIG. 6 . RADIAL DISTRIBUTION OF (a) mean axial vel.,(b) mean radial vel.

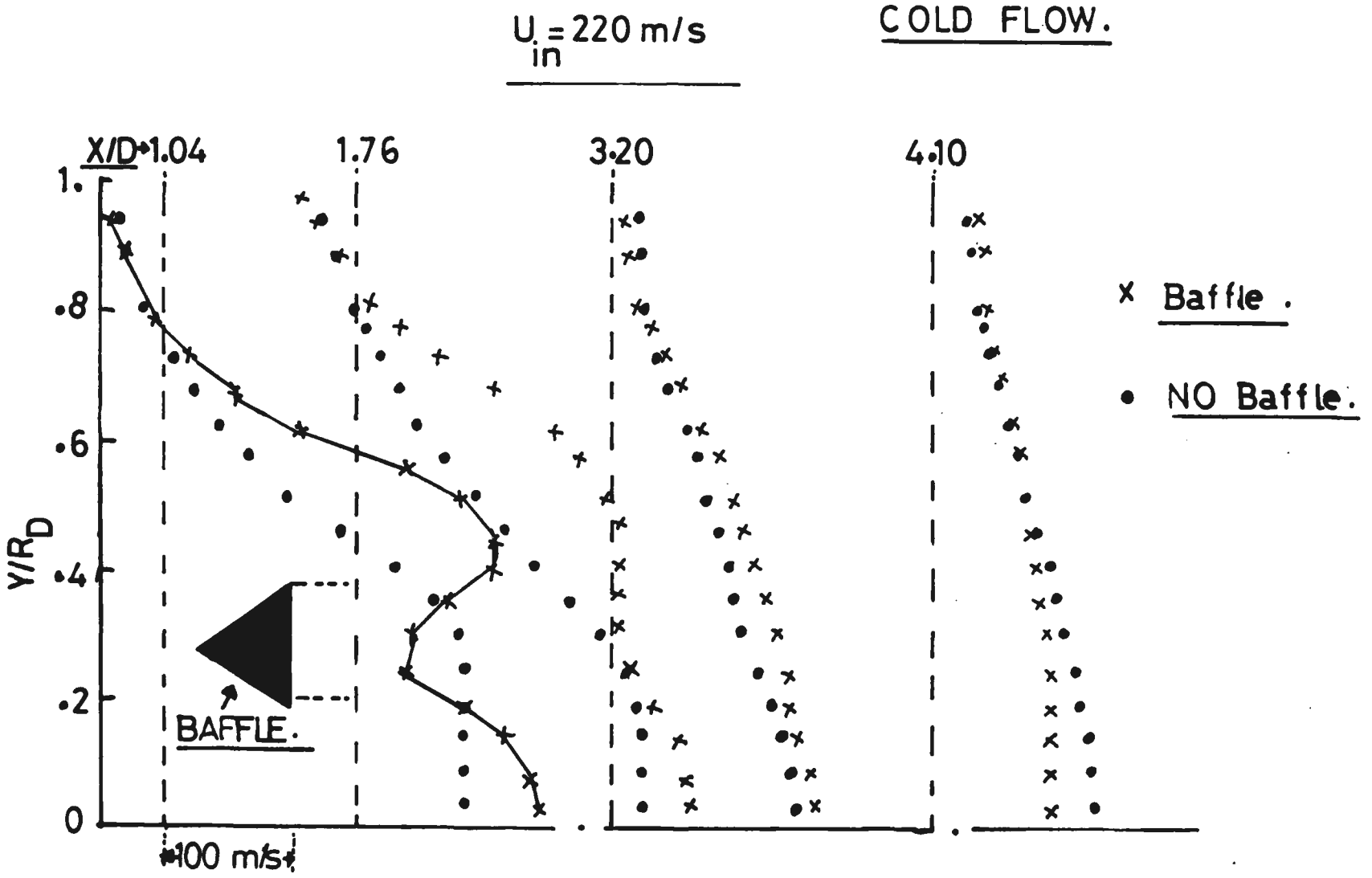

FIG. 7. RADIAL PROFILES OF AXIAL VELOCITY.

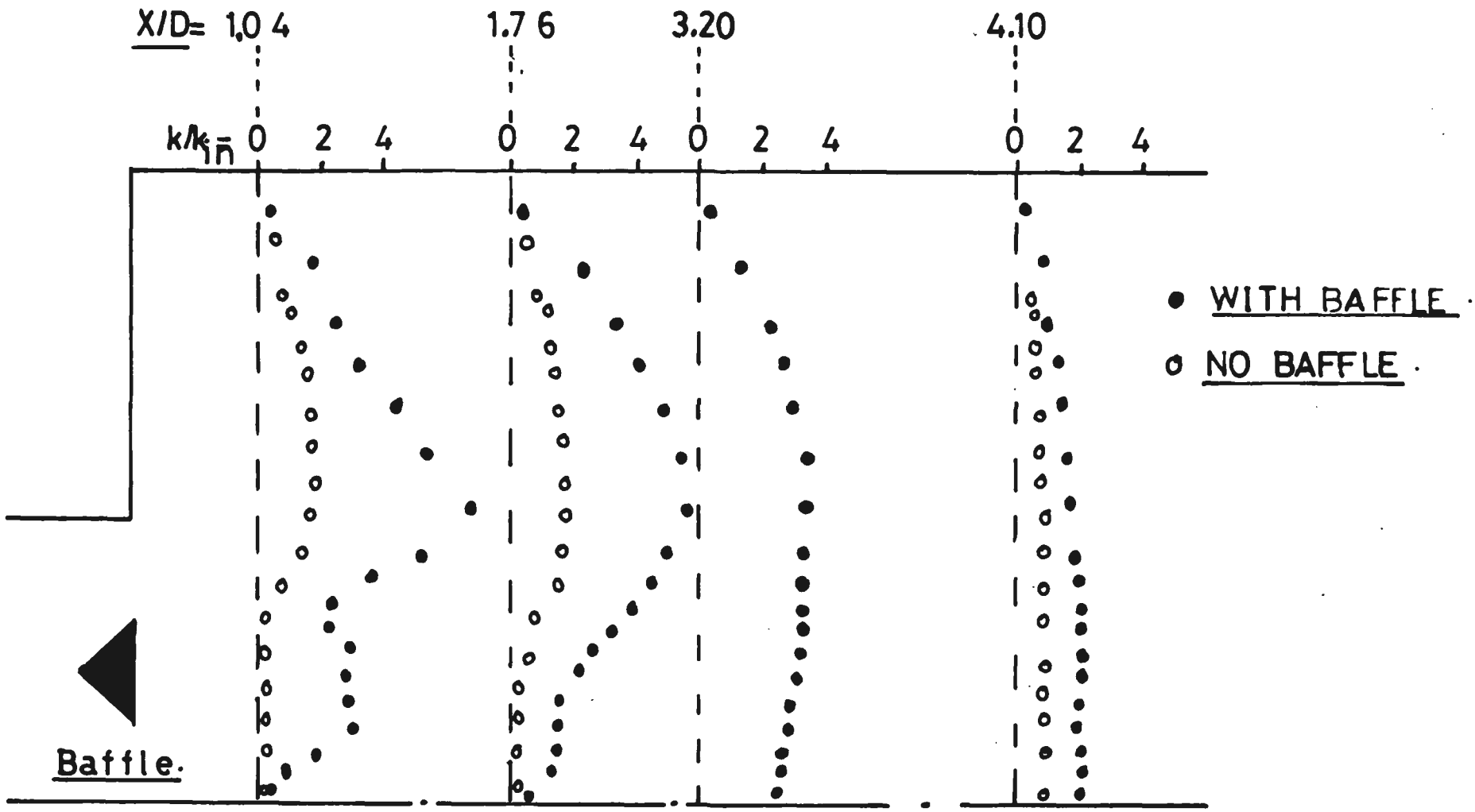

FIG. 8. RADIAL DISTRIBUTION OF MEAN KINETIC ENERGY OF TURBULENCE.

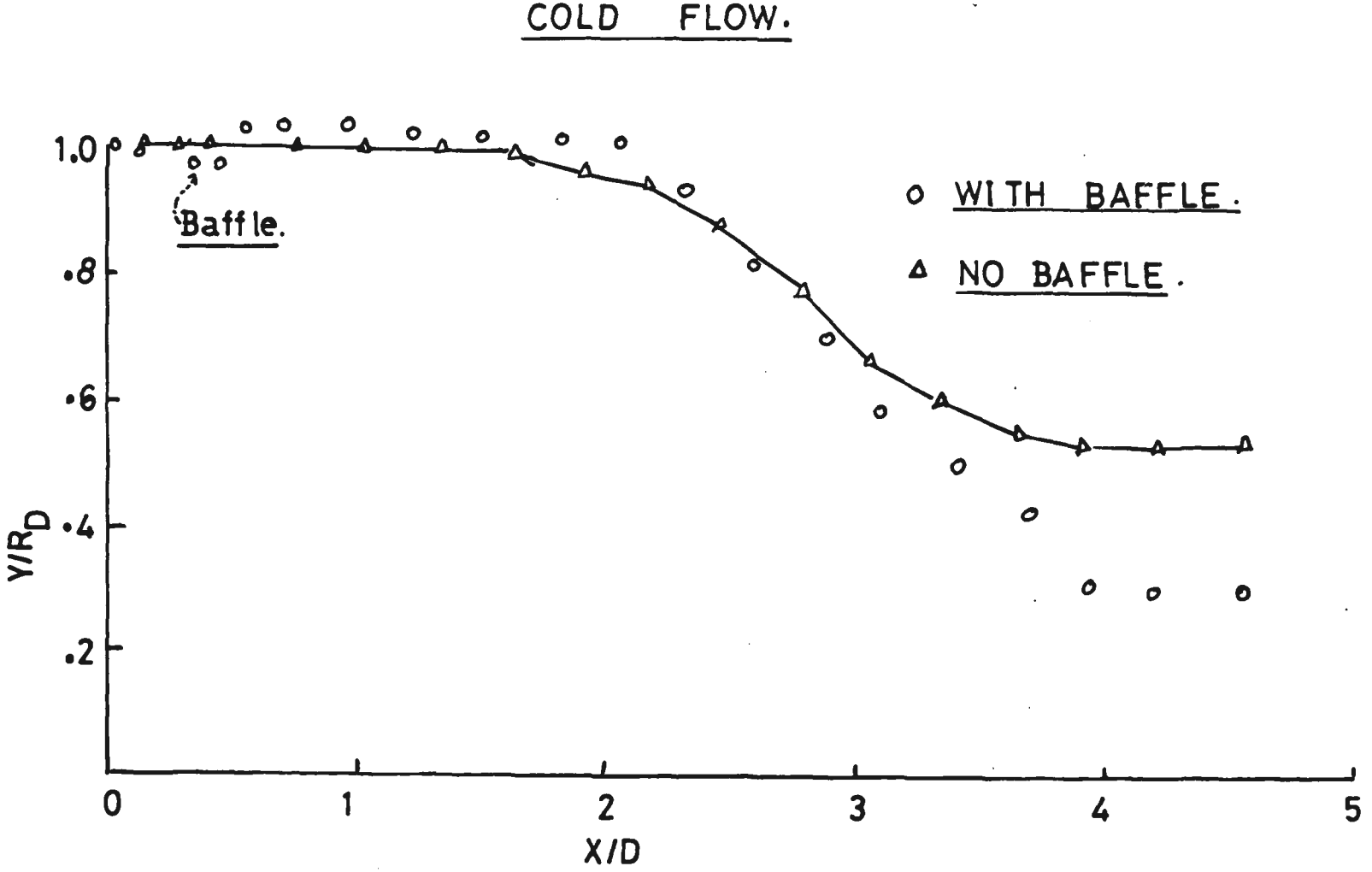

FIG. 9 . AXIAL DISTRIBUTION OF CENTRE-LINE VELOCITY.

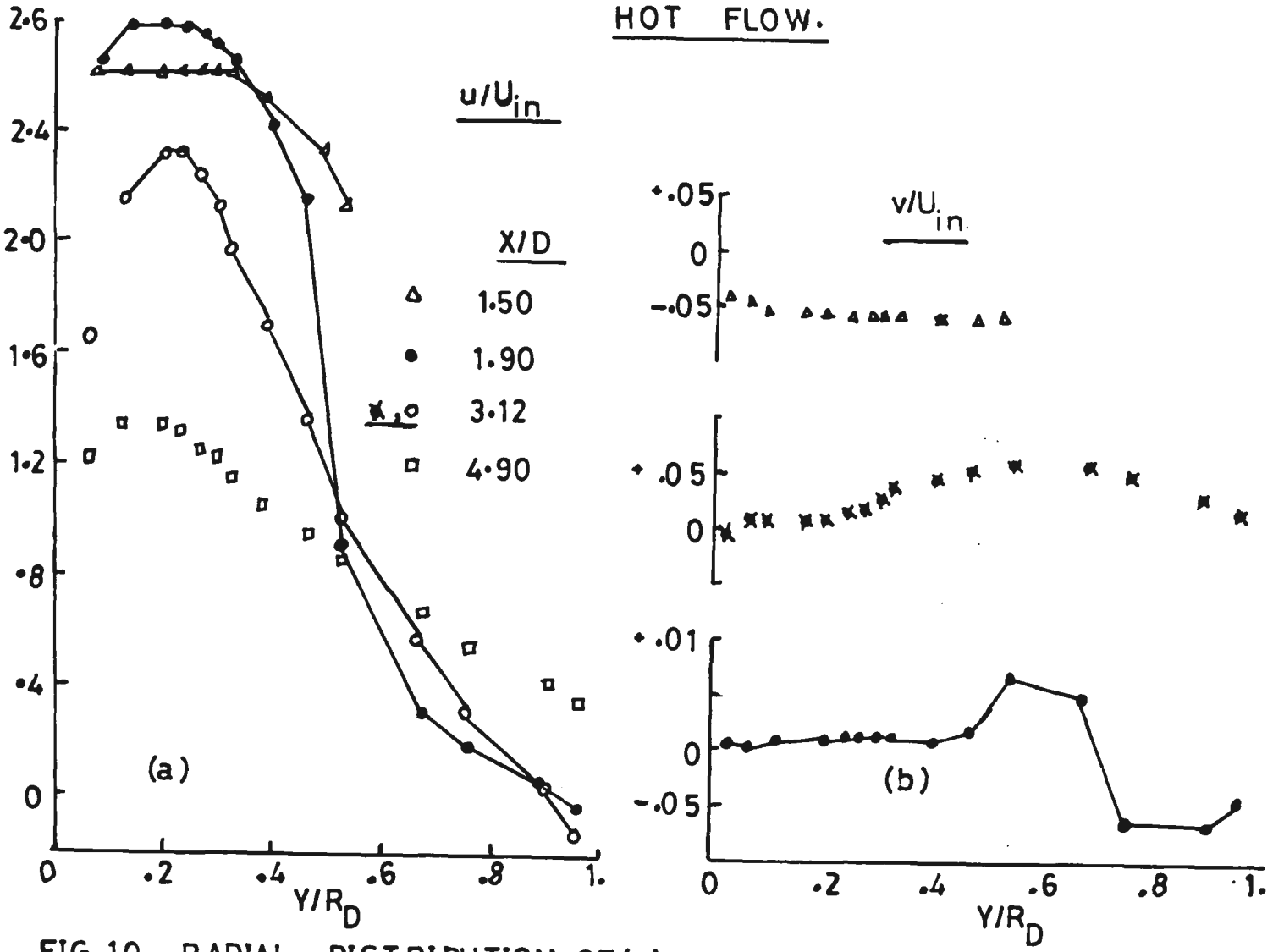

FIG. 10. RADIAL DISTRIBUTION OF (a) mean axial vel., (b) mean radial vel.

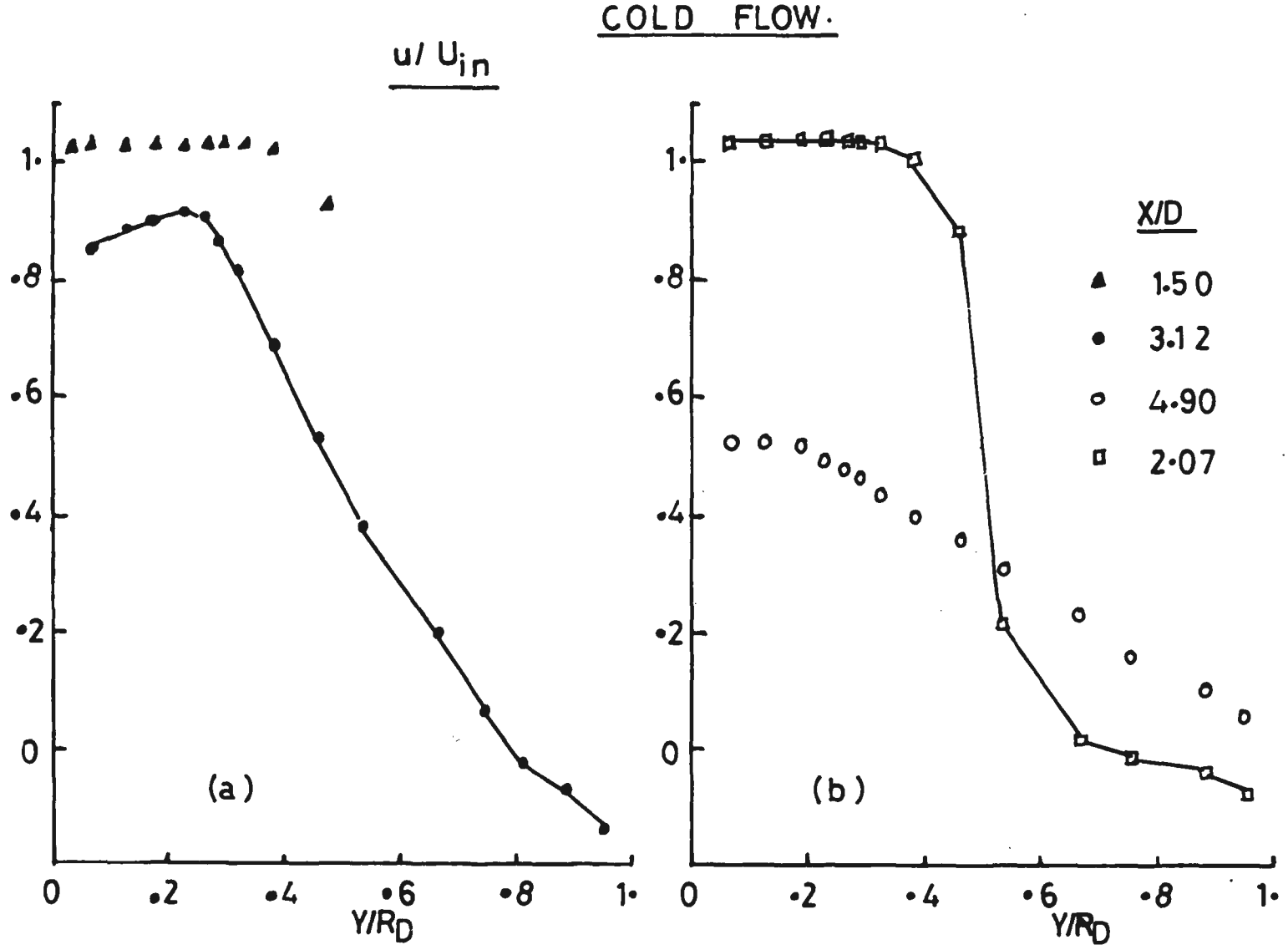

FIG. 11(a,b). RADIAL DISTRIBUTION OF MEAN AXIAL VELOCITY.

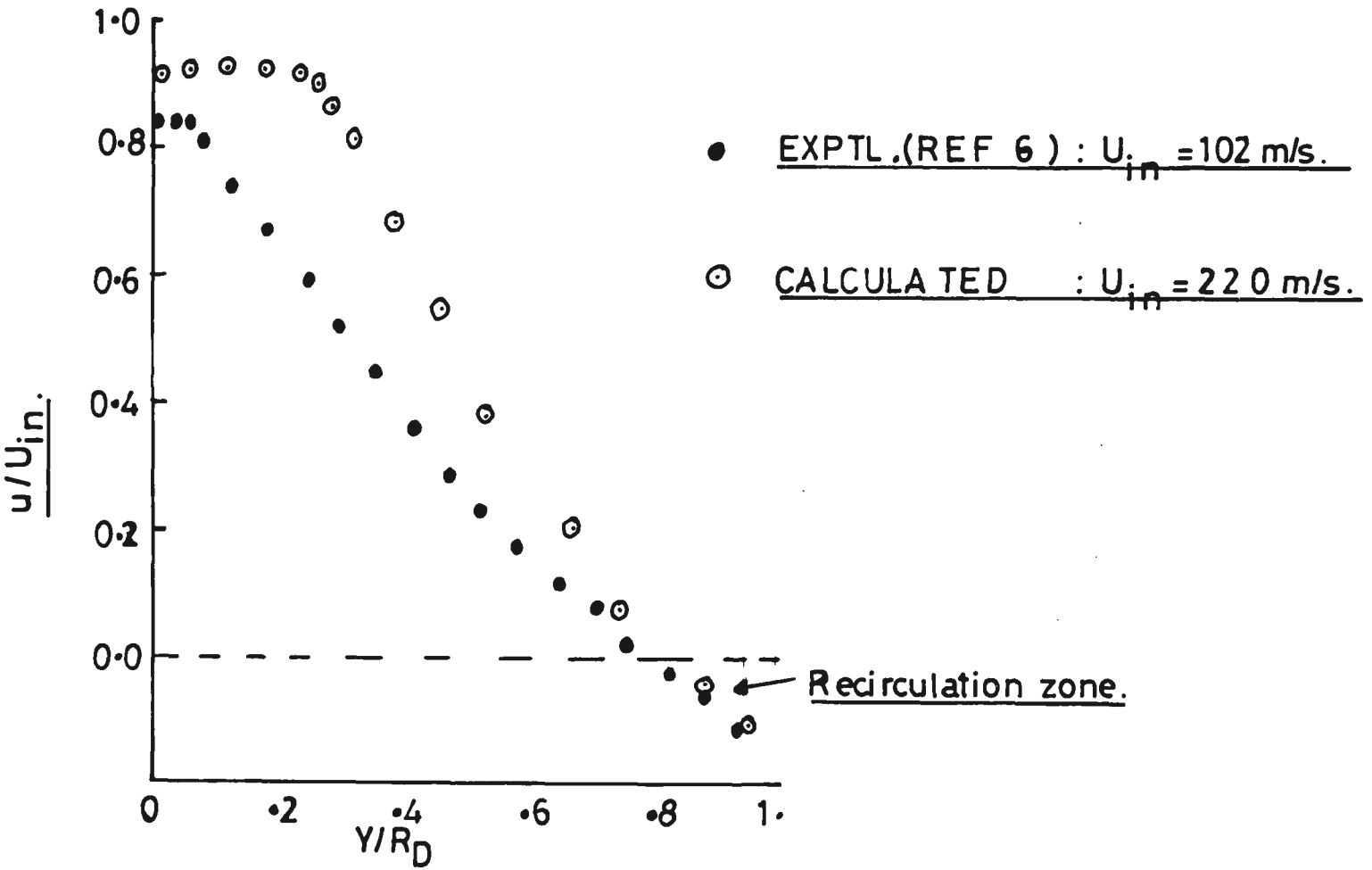

FIG·11(c). COMPARISON BETWEEN MEASURED AND CALCULATED MEAN AXIAL VELOCITY PROFILES.

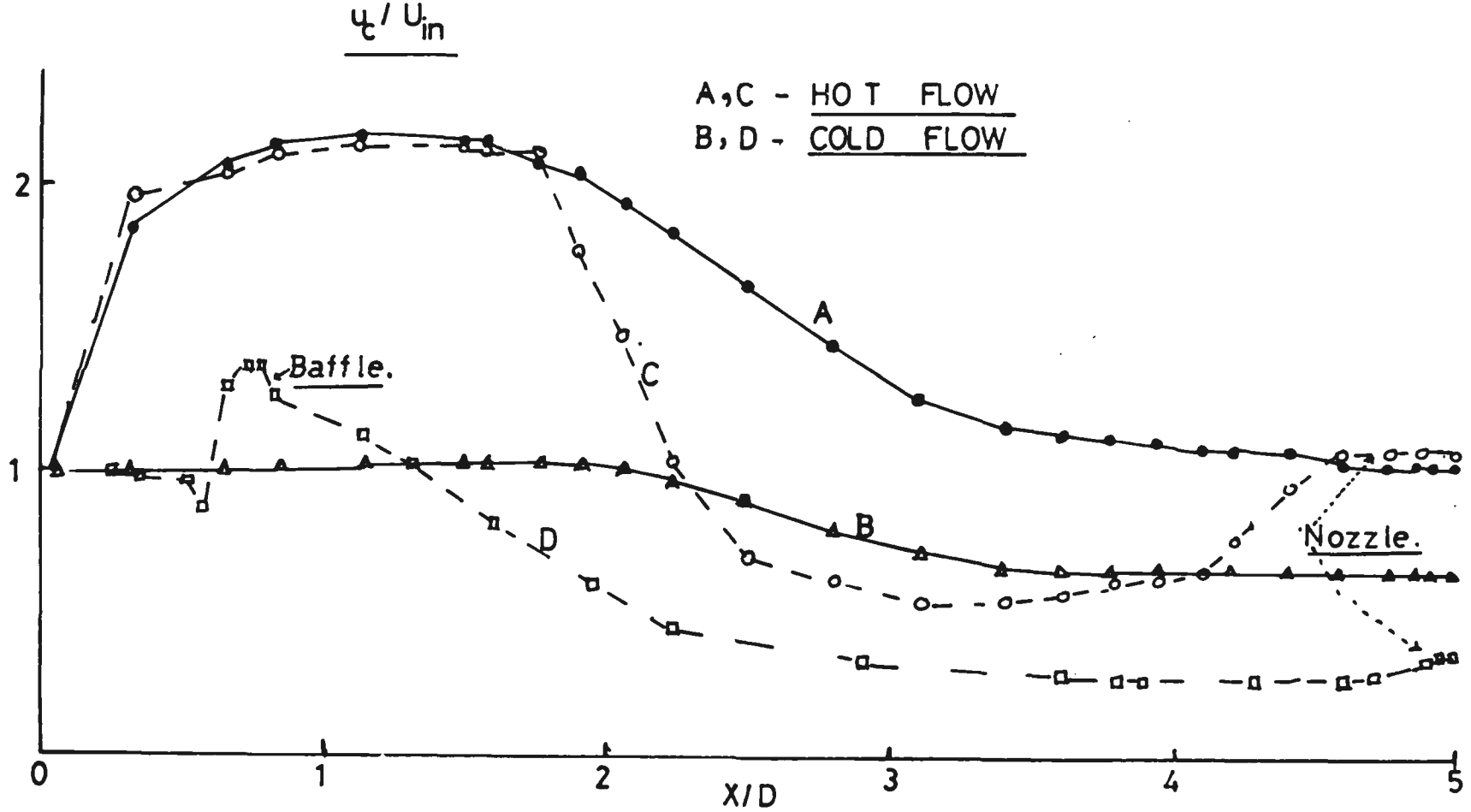

FIG. 12 . AXIAL DISTRIBUTIONS OF CENTRE-LINE VELOCITIES FOR DIFFERENT CASES.

COLD FLOW.

VELOCITY FIELD POSITION I= 4

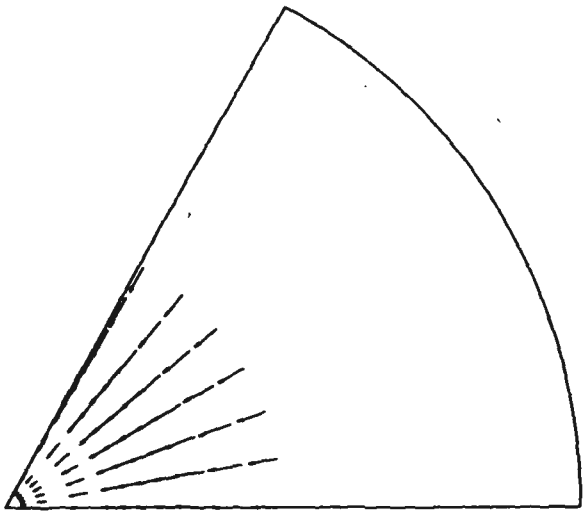

VELOCITY FIELD POSITION I= 6

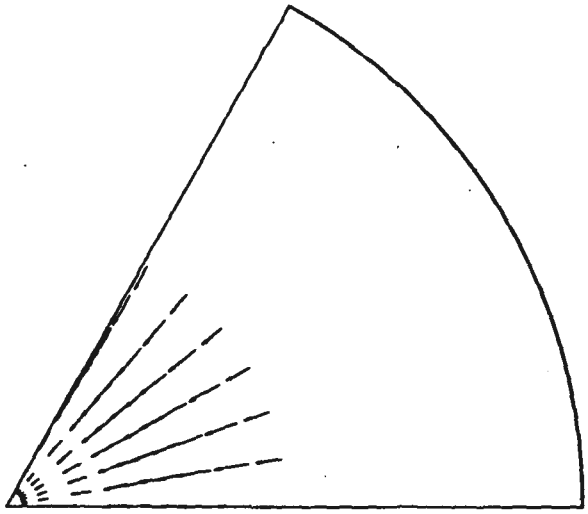

VELOCITY FIELD POSITION I= 11

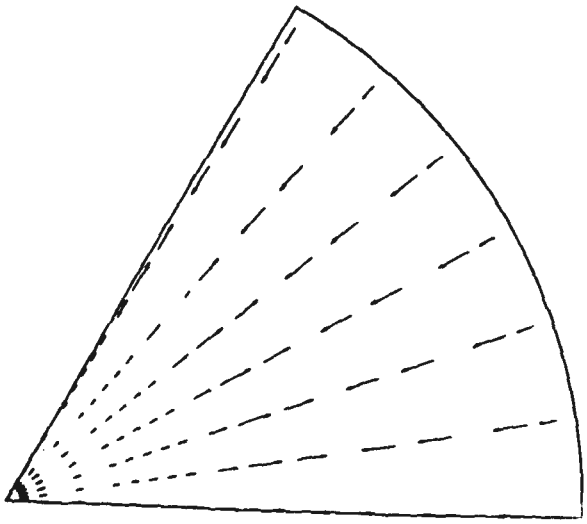

VELOCITY FIELD POSITION I= 15

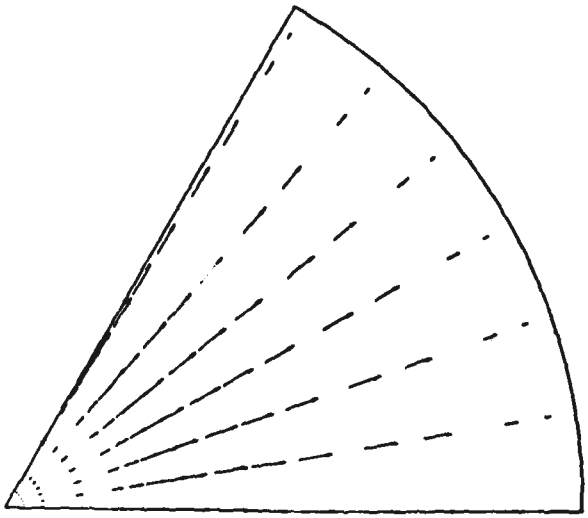

FIG.13(a). RADIAL VELOCITY VECTORS.

COLD FLOW.

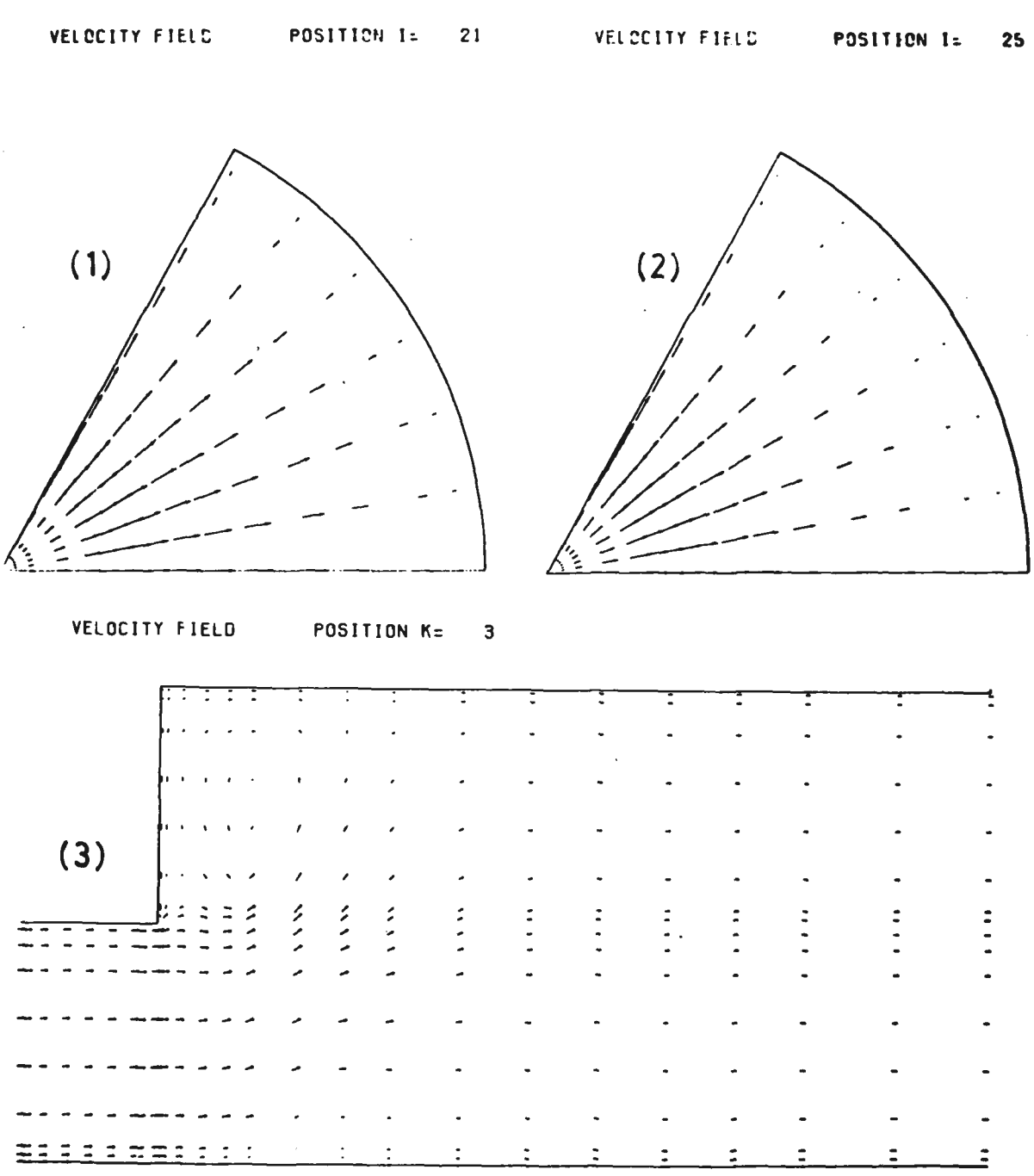

FIG. 13(b). 1,2 - RADIAL VELOCITY VECTORS.
3 - AXIAL VELOCITY VECTORS.

COLD FLOW. (with baffle and nozzle).

VELOCITY POSITION J= 6 VELOCITY POSITION J= 9

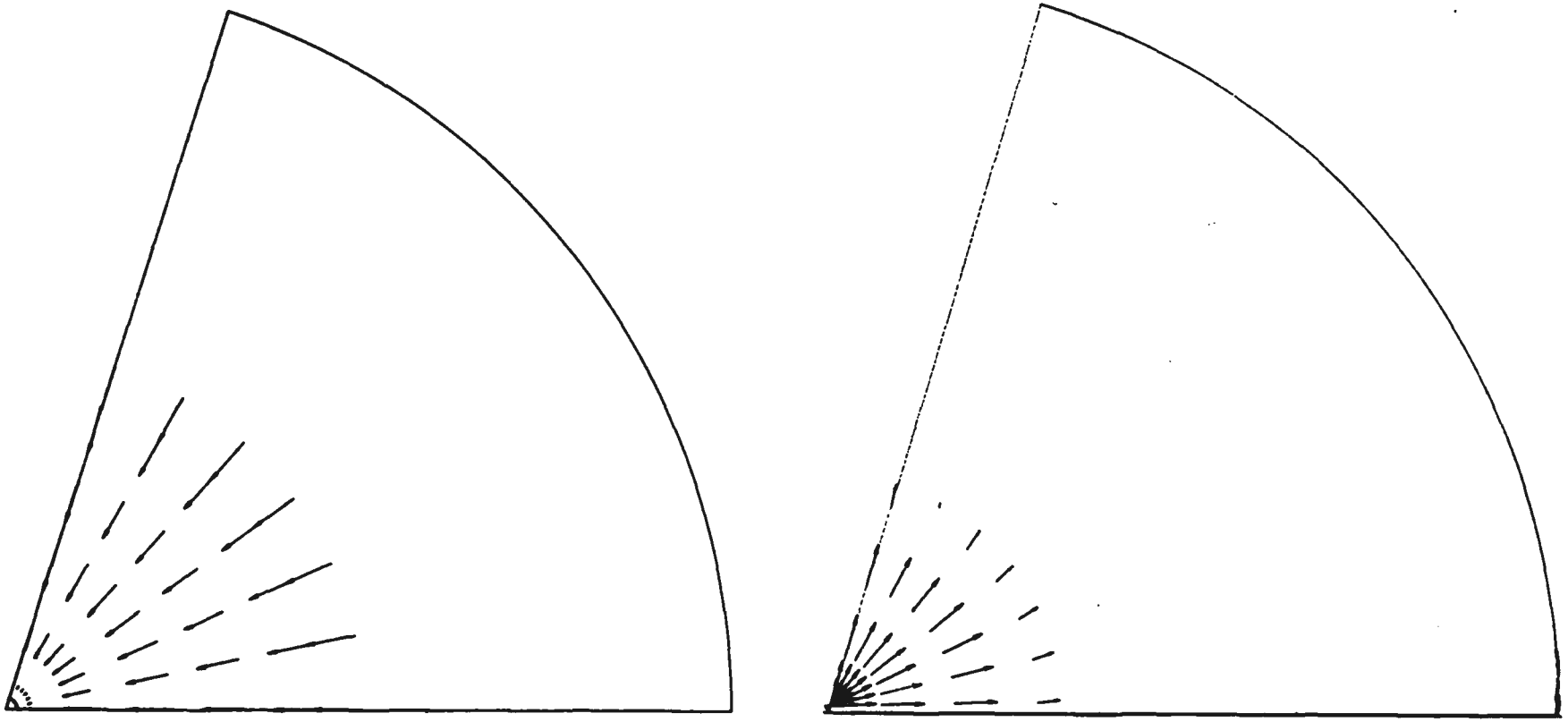

FIG.14(a). RADIAL VELOCITY VECTORS.

COLD FLOW(with baffle and nozzle).

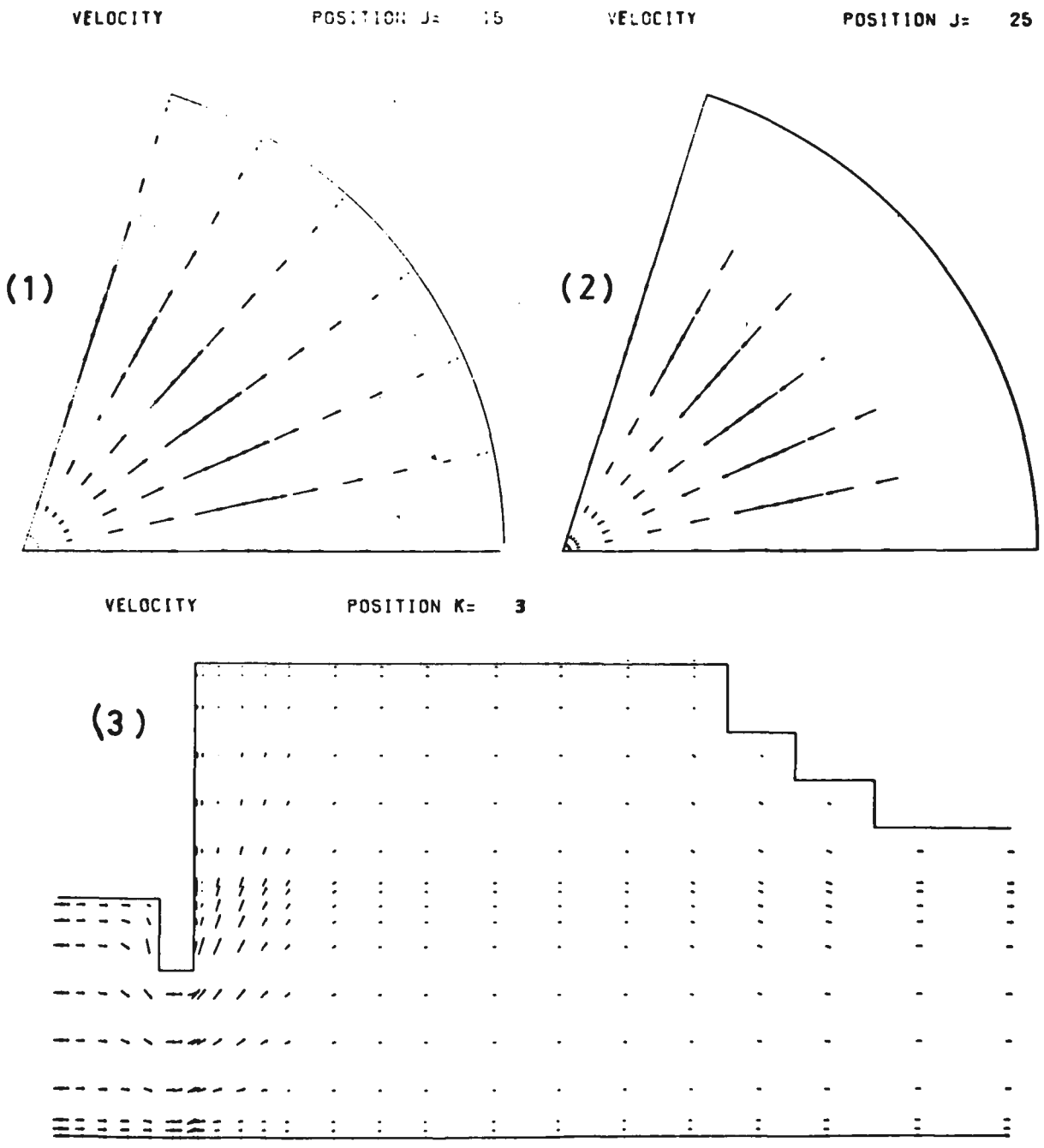

FIG 14(b) 1,2 - RADIAL VELOCITY VECTORS.
3 - AXIAL VELOCITY VECTORS.

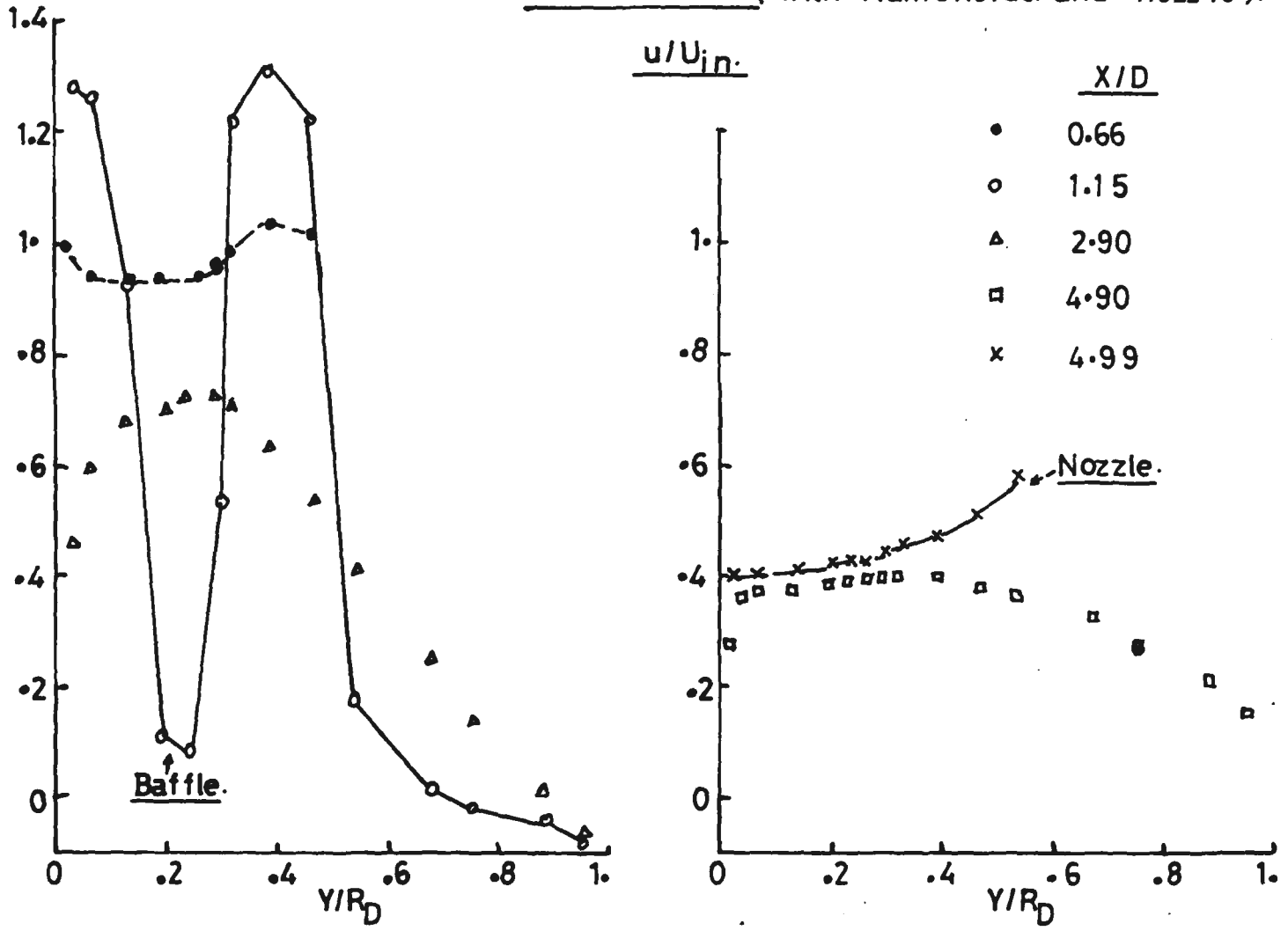

FIG. 15. RADIAL PROFILES OF MEAN AXIAL VELOCITY.

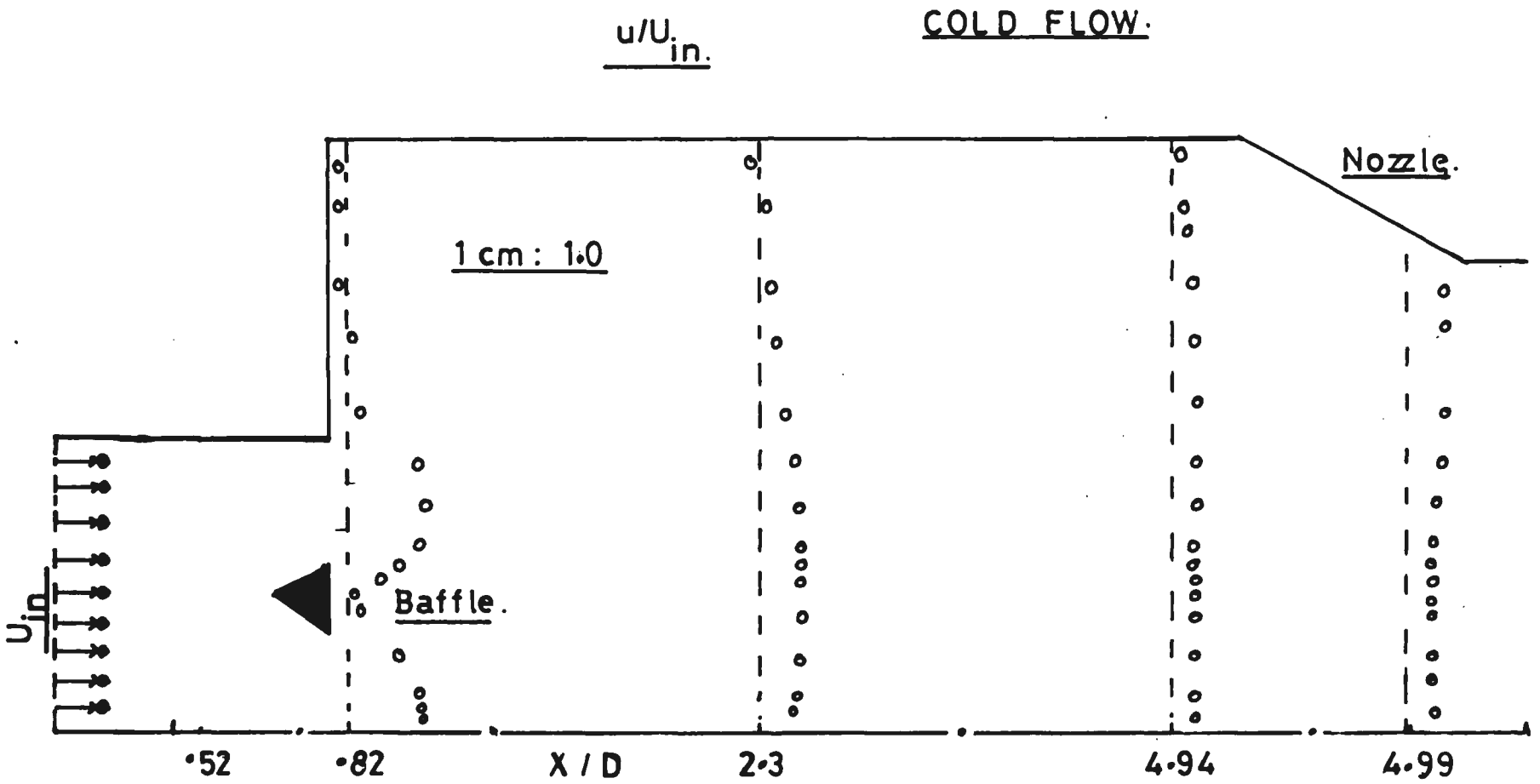

FIG.16. RADIAL DISTRIBUTIONS OF MEAN AXIAL VELOCITY.

f/a = 0.055

HOT FLOW (with flame holder and nozzle).

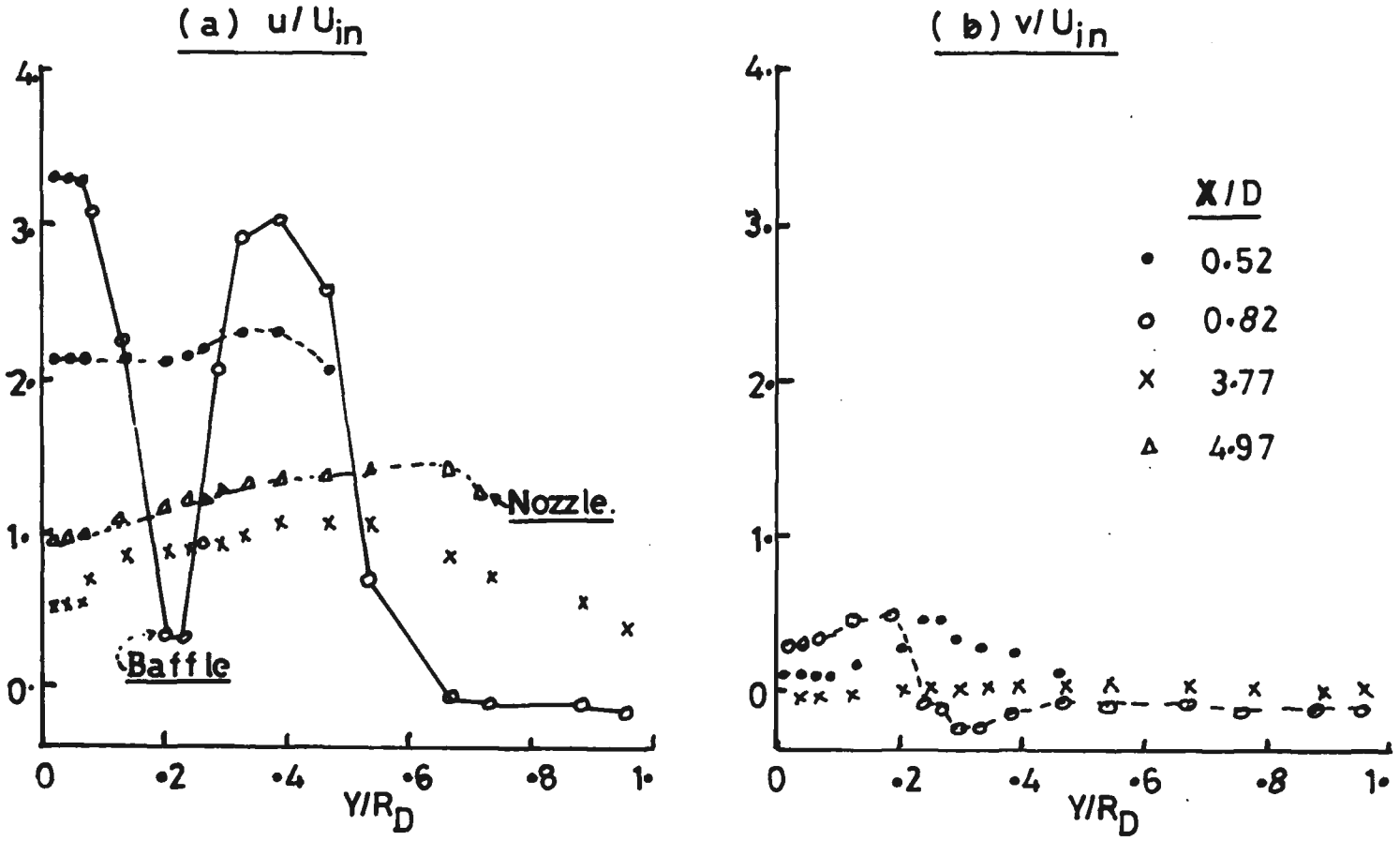

FIG.17. RADIAL DISTRIBUTIONS OF (a) mean axial vel., (b) mean radial vel. PROFILES.

HOT FLOW(with flameholder and nozzle).

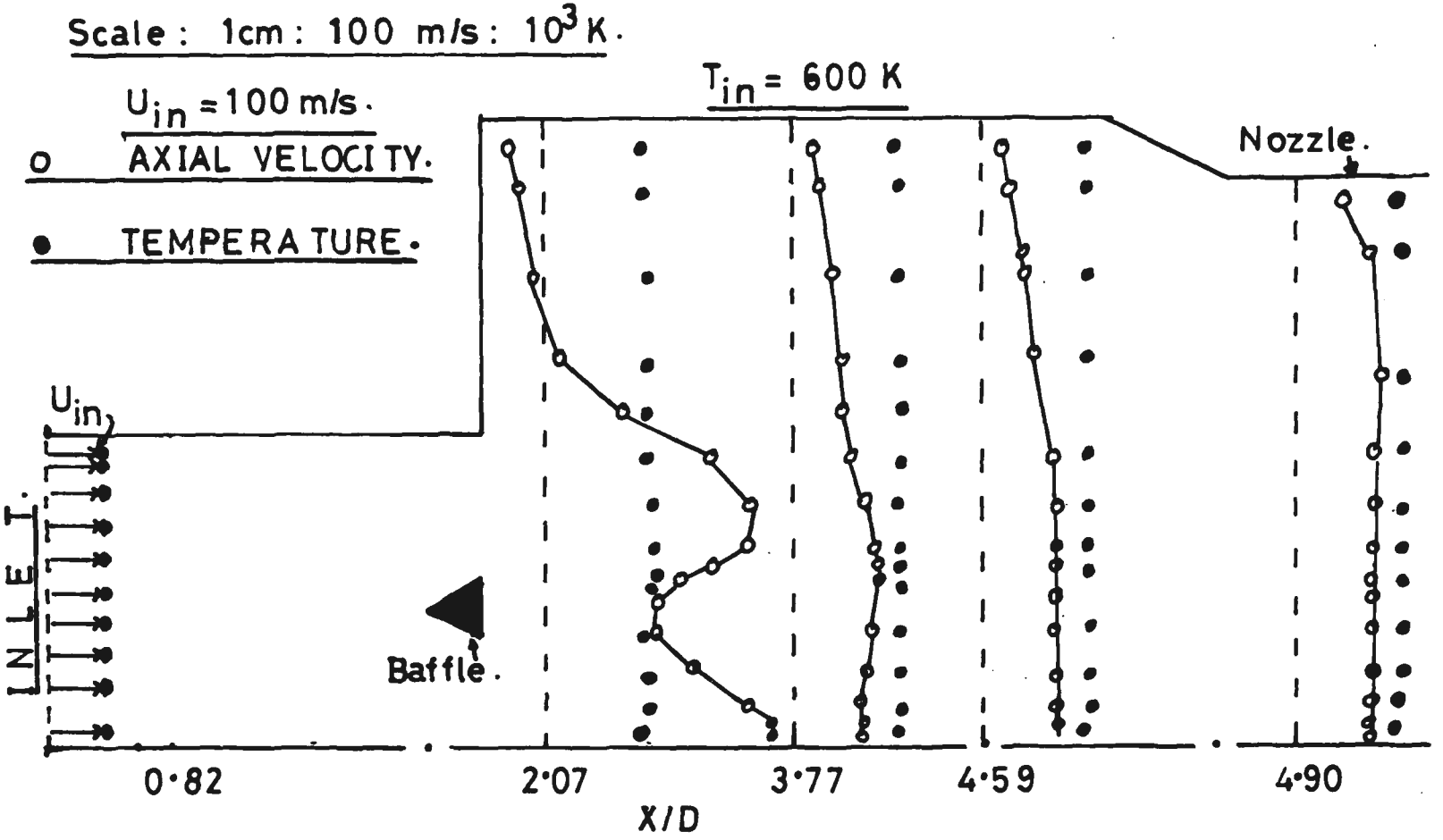

FIG.17(c). RADIAL DISTRIBUTION OF AXIAL VELOCITY AND TEMPERATURE.

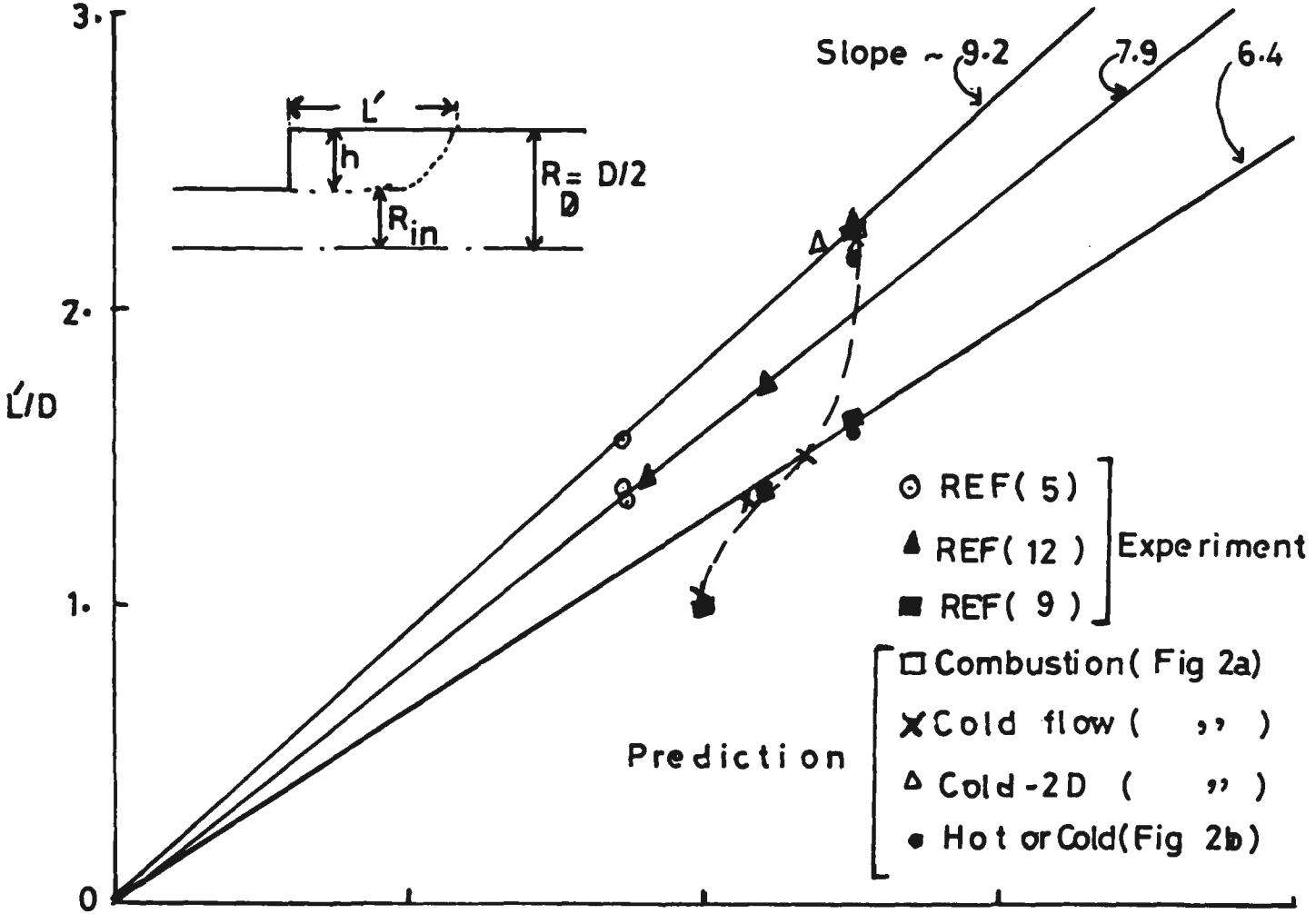

FIG·18· VARIATION OF L′ WITH h (R_{IN} CONSTANT)·

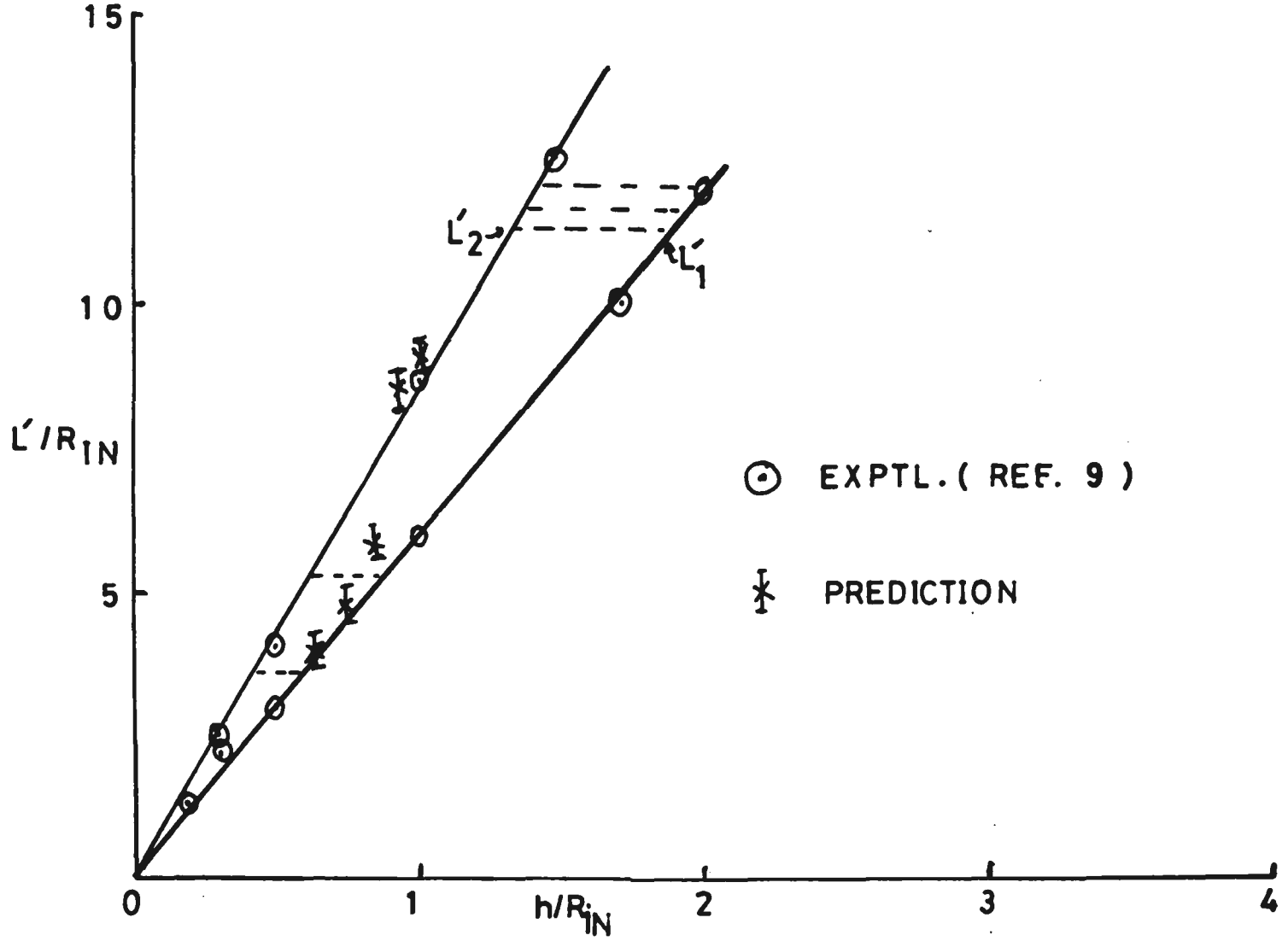

FIG. 19. VARIATION OF L' WITH h (R_{IN} CONSTANT).

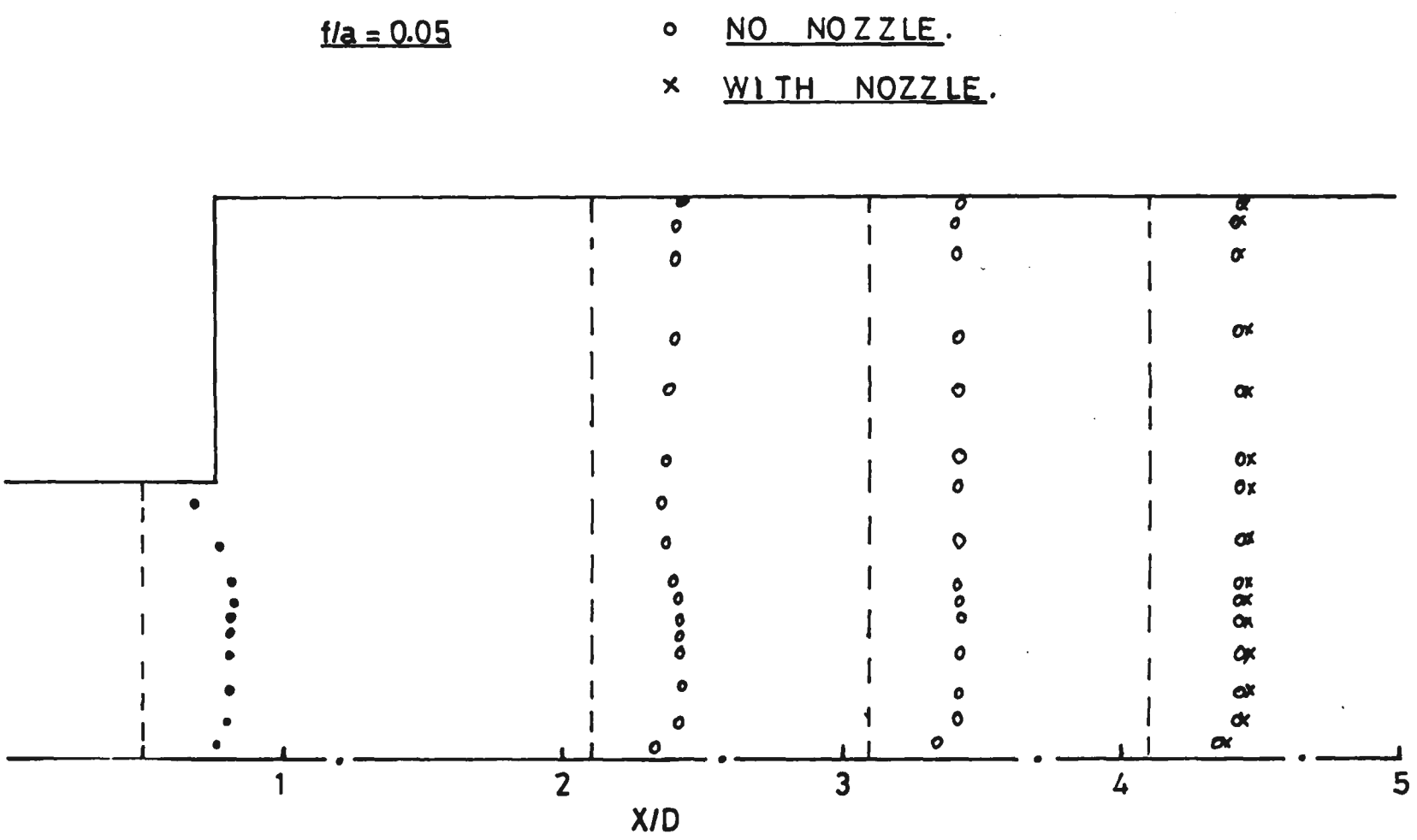

FIG.20. RADIAL DISTRIBUTIONS OF TEMPERATURE.

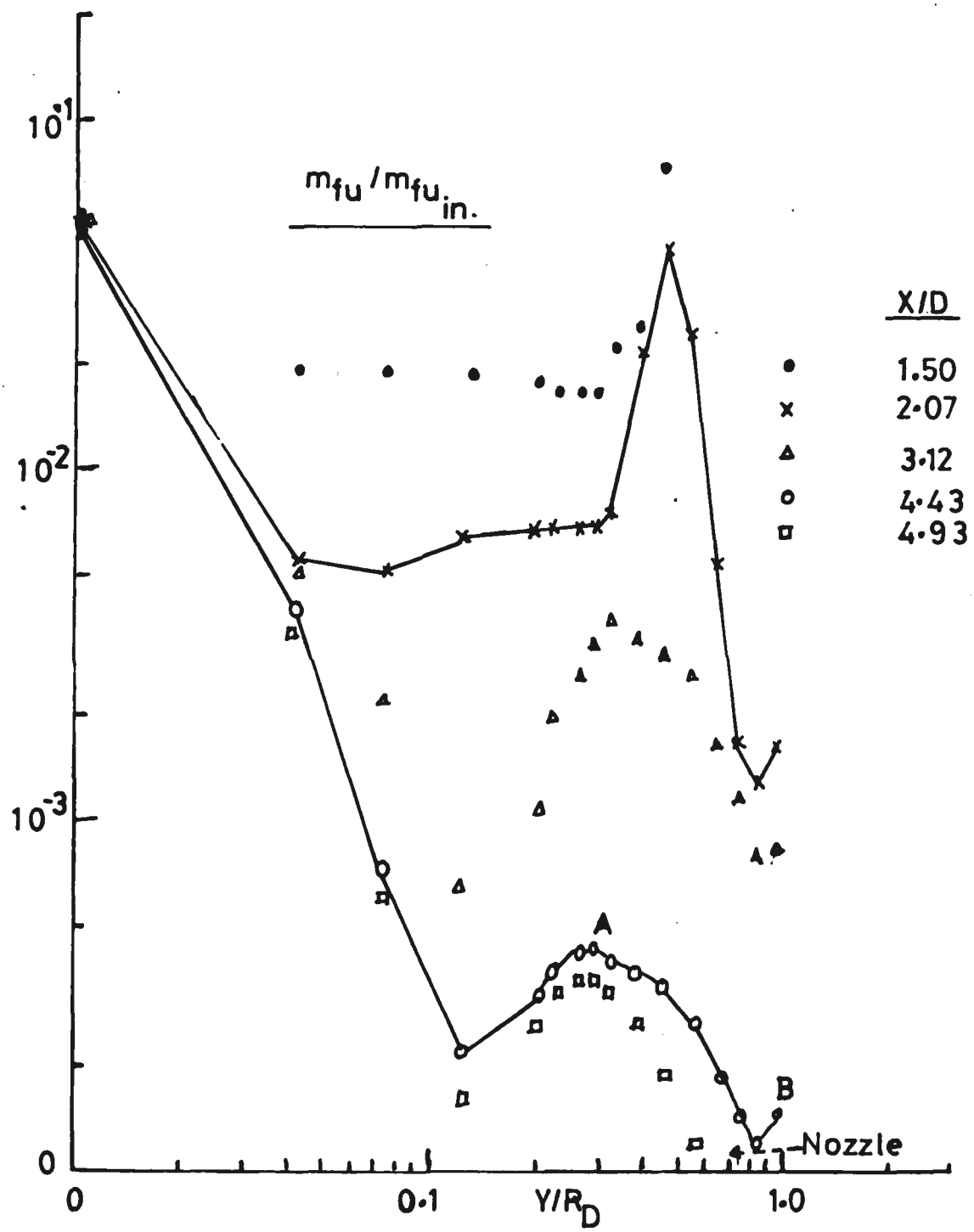

FIG·21 · RADIAL DISTRIBUTIONS OF m_{fu} .

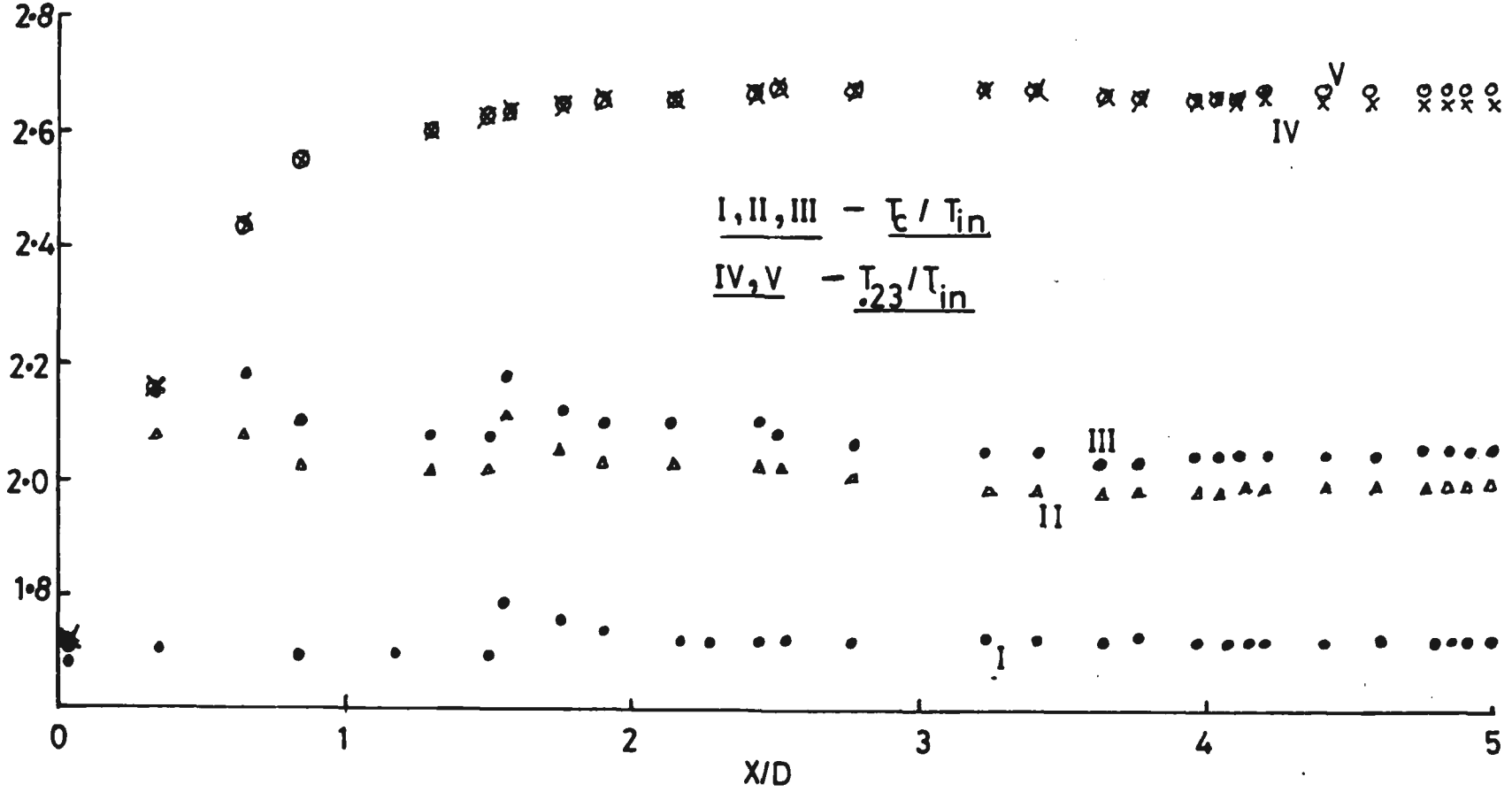

FIG.22. AXIAL DISTRIBUTIONS OF TEMPERATURE.

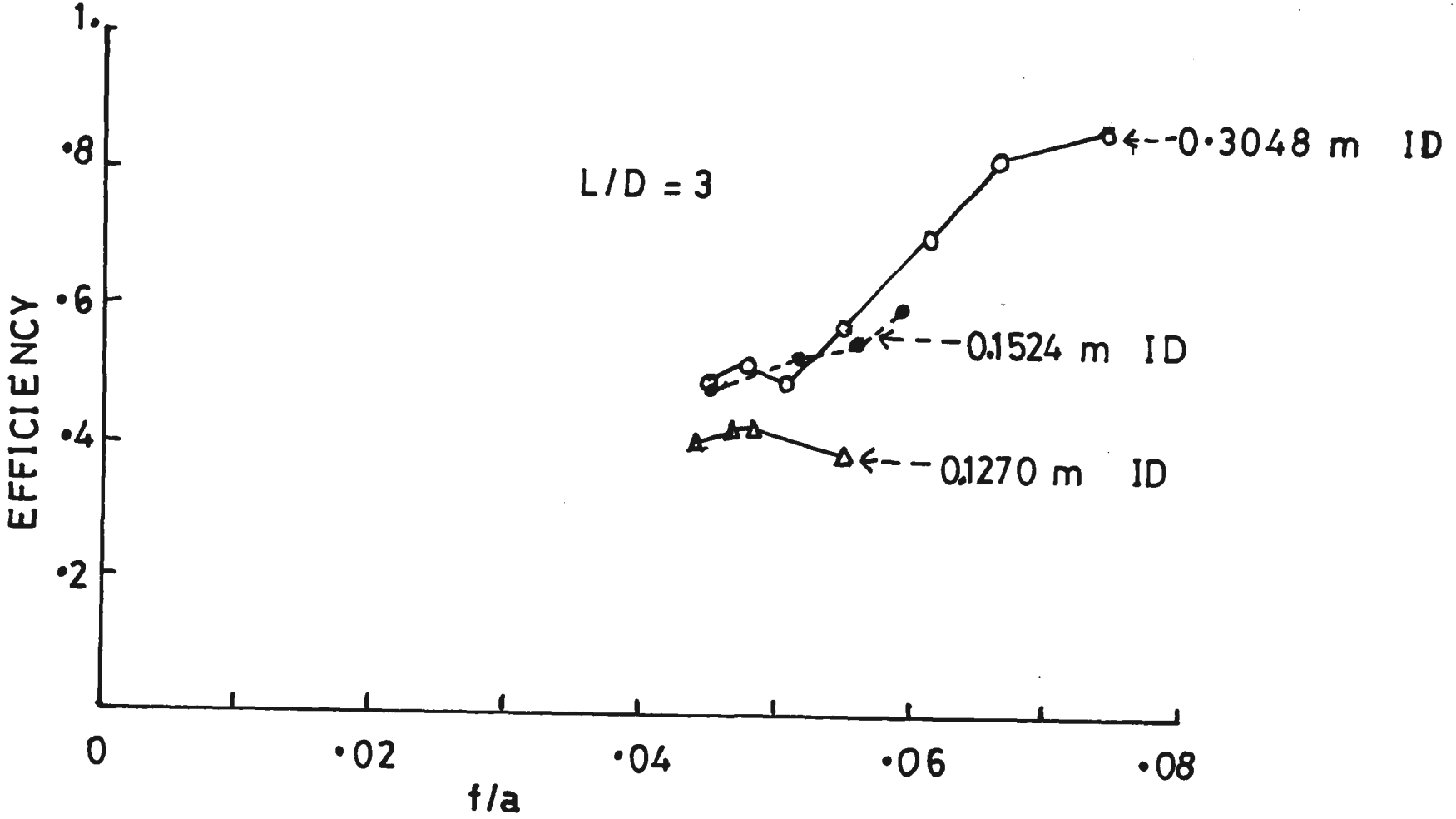

FIG·23· EFFECTS OF DUCT DIAM. AND f/a ON EFFICIENCY.

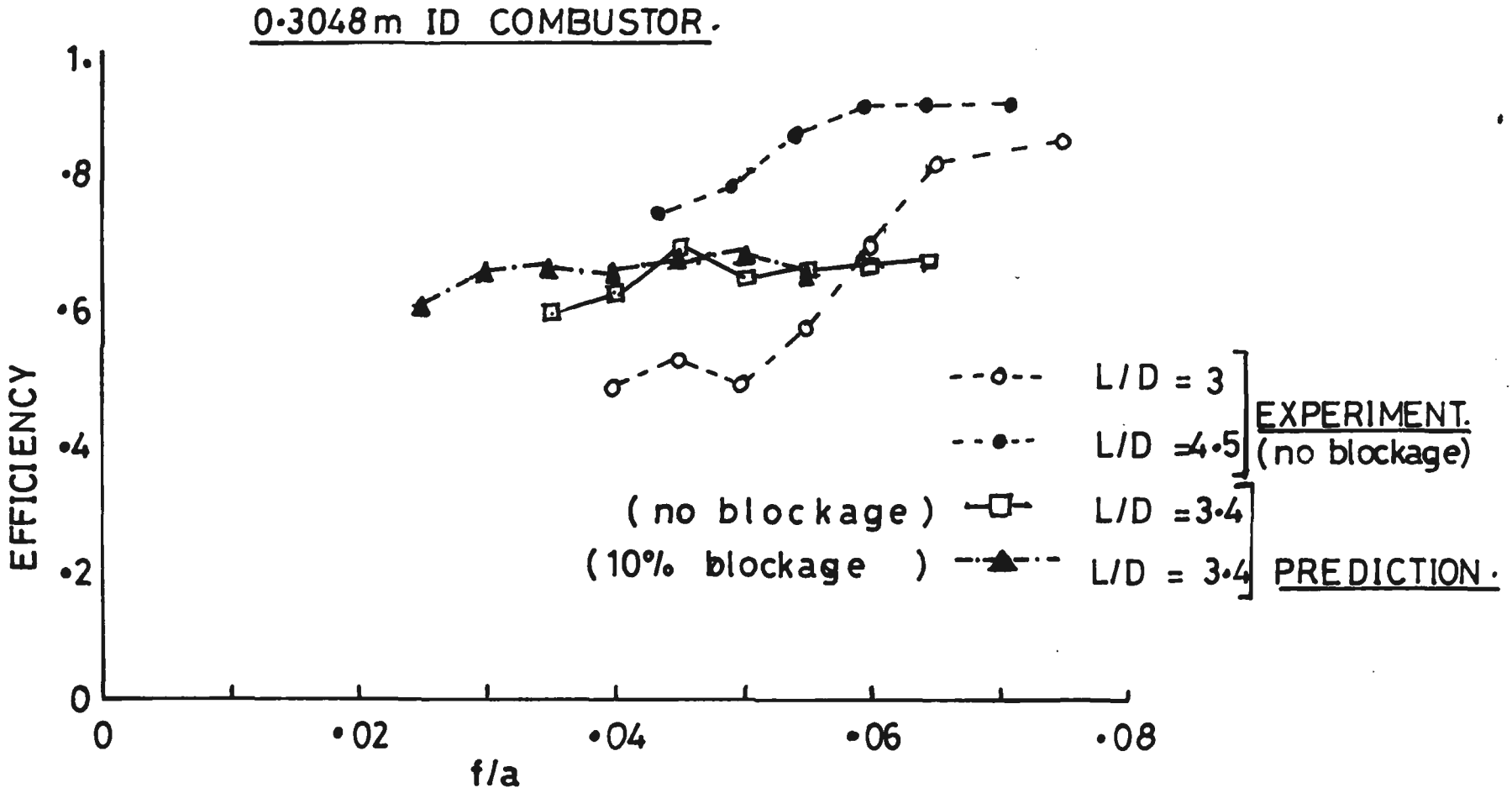

FIG·24· PREDICTED AND EXPERIMENTAL EFFICIENCY.
(PRE-MIXED FLAME)